2004-09

Performance analysis of wireless LAN signals transmitted over a ricean fading channel in a pulsed-noise preference environment

Spyrou, Evangelos

Monterey California. Naval Postgraduate School

NAVAL POSTGRADUATE SCHOOL

THESIS

PERFORMANCE ANALYSIS OF WIRELESS LAN SIGNALS TRANSMITTED OVER A RICEAN FADING CHANNEL IN A PULSED–NOISE INTERFERENCE ENVIRONMENT

by

Evangelos Spyrou

September 2004

Thesis Advisor:	R. Clark Robertson
Second Reader:	David C. Jenn

Approved for public release; distribution is unlimited

THIS PAGE INTENTIONALLY LEFT BLANK

REPORT DOCUMENTATION PAGE			Form Approved OMB No. 0704-0188
Public reporting burden for this collection of information is estimated to average 1 hour per response, including the time for reviewing instruction, searching existing data sources, gathering and maintaining the data needed, and completing and reviewing the collection of information. Send comments regarding this burden estimate or any other aspect of this collection of information, including suggestions for reducing this burden, to Washington headquarters Services, Directorate for Information Operations and Reports, 1215 Jefferson Davis Highway, Suite 1204, Arlington, VA 22202-4302, and to the Office of Management and Budget, Paperwork Reduction Project (0704-0188) Washington DC 20503.			
1. AGENCY USE ONLY ***(Leave blank)***	**2. REPORT DATE** September 2004	**3. REPORT TYPE AND DATES COVERED** Master's Thesis	
4. TITLE AND SUBTITLE: Performance Analysis of Wireless LAN Signals Transmitted Over a Ricean Fading Channel in a Pulsed–Noise Interference Environment			**5. FUNDING NUMBERS**
6. AUTHOR(S) Evangelos Spyrou			
7. PERFORMING ORGANIZATION NAME(S) AND ADDRESS(ES) Naval Postgraduate School Monterey, CA 93943-5000			**8. PERFORMING ORGANIZATION REPORT NUMBER**
9. SPONSORING /MONITORING AGENCY NAME(S) AND ADDRESS(ES) N/A			**10. SPONSORING/MONITORING AGENCY REPORT NUMBER**
11. SUPPLEMENTARY NOTES The views expressed in this thesis are those of the author and do not reflect the official policy or position of the Department of Defense or the U.S. Government.			
12a. DISTRIBUTION / AVAILABILITY STATEMENT Approved for public release; distribution is unlimited			**12b. DISTRIBUTION CODE**

13. ABSTRACT (maximum 200 words)

This thesis examines the performance of the waveforms specified by the *IEEE 802.11a* wireless local area network standard when the signal is transmitted over a Ricean fading channel with AWGN and pulsed–noise interference. The pulsed interference is assumed to have constant average power and is either fading or non-fading. The probability of bit error is conditional on the received signal–to–noise power ratio, which is modeled as a random variable. The probability density function of this random variable is obtained either analytically or numerically for each modulation type, and the probability of bit error is evaluated as the expected value of the conditional probability. In one case, use is made of a new technique for the numerical inverse of the Laplace transform in order to evaluate numerically the signal–to–noise ratio probability density function. Due to the complexity of the analysis when both the signal and the interference are subject to Ricean fading, the analysis was simplified by assuming Ricean signal fading with Rayleigh interference fading and vice versa. The results of the analysis show that performance is affected by the degree of signal fading and also depends on the pulsed interference duty cycle. The signal–to–interference power ratio affects the way performance depends on these two factors.

14. SUBJECT TERMS IEEE 802.11a, Wireless, Local Area Network, Signal–to–Noise Power Ratio, Ricean Fading Channel, Rayleigh Interference Signal Fading, Signal–to–Interference Power Ratio, Probability Density Function, AWGN, Pulsed–Noise Interference			**15. NUMBER OF PAGES** 91
			16. PRICE CODE
17. SECURITY CLASSIFICATION OF REPORT Unclassified	**18. SECURITY CLASSIFICATION OF THIS PAGE** Unclassified	**19. SECURITY CLASSIFICATION OF ABSTRACT** Unclassified	**20. LIMITATION OF ABSTRACT** UL

NSN 7540-01-280-5500

Standard Form 298 (Rev. 2-89)
Prescribed by ANSI Std. 239-18

THIS PAGE INTENTIONALLY LEFT BLANK

Approved for public release; distribution is unlimited

PERFORMANCE ANALYSIS OF WIRELESS LAN SIGNALS TRANSMITTED OVER A RICEAN FADING CHANNEL IN A PULSED–NOISE INTERFERENCE ENVIRONMENT

Evangelos Spyrou
Captain, Hellenic Air Force
B.S.E.E., Hellenic Air Force Academy, 1992

Submitted in partial fulfillment of the
requirements for the degree of

MASTER OF SCIENCE IN ELECTRICAL ENGINEERING
and
MASTER OF SCIENCE IN SYSTEMS ENGINEERING

from the

NAVAL POSTGRADUATE SCHOOL
September 2004

Author: Evangelos Spyrou

Approved by: R. Clark Robertson
Thesis Advisor

David C. Jenn
Second Reader

Dan C. Boger
Chairman, Department of Information Science

John P. Powers
Chairman, Department of Electrical and Computer Engineering

THIS PAGE INTENTIONALLY LEFT BLANK

ABSTRACT

This thesis examines the performance of the waveforms specified by the *IEEE 802.11a* wireless local area network standard when the signal is transmitted over a Ricean fading channel with AWGN and pulsed–noise interference. The pulsed interference is assumed to have constant average power and is either fading or non-fading. The probability of bit error is conditional on the received signal–to–noise power ratio, which is modeled as a random variable. The probability density function of this random variable is obtained either analytically or numerically for each modulation type, and the probability of bit error is evaluated as the expected value of the conditional probability. In one case, use is made of a new technique for the numerical inverse of the Laplace transform in order to evaluate numerically the signal–to–noise ratio probability density function. Due to the complexity of the analysis when both the signal and the interference are subject to Ricean fading, the analysis was simplified by assuming Ricean signal fading with Rayleigh interference fading and vice versa. The results of the analysis show that performance is affected by the degree of signal fading and also depends on the pulsed interference duty cycle. The signal–to–interference power ratio affects the way performance depends on these two factors.

THIS PAGE INTENTIONALLY LEFT BLANK

TABLE OF CONTENTS

THIS PAGE INTENTIONALLY LEFT BLANK

LIST OF FIGURES

LIST OF TABLES

THIS PAGE INTENTIONALLY LEFT BLANK

ACKNOWLEDGMENTS

For the completion of this thesis, I would like to gratefully thank my thesis advisor Professor R. Clark Robertson. His deep insight in the subject under study and his continuous guidance helped me take my work to a fruitful end and made my effort a meaningful learning experience.

I would also like to thank Professor David C. Jenn, second reader of my thesis.

Finally, I would like to thank all the people who encouraged me and contributed in any way to the fulfillment of my postgraduate studies. Primarily, among those, my wife Athanasia.

THIS PAGE INTENTIONALLY LEFT BLANK

EXECUTIVE SUMMARY

The objective of this thesis was to investigate the performance of wireless local area networks implemented according to the *IEEE 802.11a* standard when the signal is transmitted over a Ricean fading channel with AWGN and noise–like, pulsed interference.

Initially, we assumed that only the signal was affected by fading. In order to evaluate the performance under these channel conditions, we utilized analytic expressions derived in a previous work that describe performance when the signal is transmitted over a Ricean fading channel with AWGN. These formulas where modified to accommodate the presence of noise–like interference in the channel, and then they were used to numerically evaluate the performance in terms of the probability of bit error. Both the non–coded and coded cases were examined. Also, both hard decision and soft decision decoding were investigated. Quite crucial for the numerical evaluation of the performance with soft decision decoding was the numerical inverse of the two–sided Laplace transform. The results of the analysis indicated that performance depends on the degree of signal fading and on the pulsed interference duty cycle.

Next, we assumed that both the transmitted signal and the noise–like interference are subject to Ricean fading and that the interference power is significantly greater than the AWGN power. The attempt to evaluate the performance for the general case proved quite complicated. Therefore, we examined two specific cases, which simplified the complicated general case. Specifically, we investigated the performance when the signal encounters Rayleigh fading and the interference is subject to Ricean fading, and when the signal is subject to Ricean fading and the interference subject to Rayleigh fading. We examined both the non–coded and the coded case, but the investigation of the coded signal performance was limited to hard decision decoding due to the complexity of computing performance with soft decision decoding. For the first case, the analysis showed performance dependence on the interference duty cycle, but not on the degree of the interference

fading. In the second case, the investigation indicated that performance depends on the degree of signal fading and on the pulsed interference duty cycle in a way similar to the case of non–fading interference.

I. INTRODUCTION

A. OBJECTIVE

The *IEEE 802.11a* wireless local area network (WLAN) standard is one of the predominant WLAN standards. It supports variable bit rates up to 54 Mbits/sec and has been adopted by many users in various fields, both military and civilian.

The objective of this thesis was to investigate the performance of this WLAN standard when the signal is transmitted over a fading channel with additive white Gaussian noise (AWGN) and noise–like interference. The fluctuation of the received signal due to fading is modeled with the Ricean distribution. The interference signal is assumed to be turned on and off systematically (i.e., pulsed) with constant mean power, which makes the instantaneous interference power inversely proportional to the interference duty cycle (or, equivalently, the instantaneous signal–to–interference power ratio directly proportional to the interference duty cycle). Both cases of non–fading and fading interference were investigated to the extent that the complexity of the analysis for each case made that feasible.

B. RELATED RESEARCH

The performance of an *IEEE 802.11a* receiver for signal transmitted over a Nakagami fading channel with AWGN has been investigated in [1]. In [2] the performance of *IEEE 802.11a* receivers was evaluated for a signal transmitted over a Nakagami fading channel with AWGN and non–fading, pulsed noise–like interference. This work was extended in [3] which examined the performance of *IEEE 802.11a* receivers for signals transmitted over a Nakagami fading channel with AWGN and fading, pulsed noise–like interference.

In [4] Kao investigated the performance of *IEEE 802.11a* receivers when the signal is transmitted over a Ricean fading channel with AWGN. This thesis is based on his findings and extends the evaluation to the case of a Ricean fading channel with AWGN and pulsed, noise–like interference when the interference is non–fading or fading.

C. THESIS ORGANIZATION

This thesis is divided into five chapters. Following this introduction, Chapter II presents a short review of relevant theory; specifically, the Ricean distribution and the properties of the waveforms specified by the *IEEE 802.11a* standard. In Chapter III we evaluate the performance of each waveform when the signal is transmitted over a Ricean fading channel with AWGN and pulsed, noise–like interference. We examine both the non–coded and the coded case. In Chapter IV we investigate the performance of each waveform when, apart from the transmitted signal, the pulsed, noise–like interference is also subject to Ricean fading. Due to the complexity of the analysis, the evaluation in Chapter IV is limited to two specific cases (Rayleigh signal fading with Ricean interference fading and Ricean signal fading with Rayleigh interference fading), and we examine only hard decision decoding for the coded case. Finally, in Chapter V the findings are summarized along with some recommendations for further research.

II. THEORY REVIEW

A. INTRODUCTION

This chapter contains a brief review of the Ricean distribution, which is used in this thesis to model the fading channel, along with a description of the *IEEE 802.11a* waveforms' modulation and encoding.

B. THE RICEAN FADING MODEL

The Ricean fading model, which we selected for our study, is used when a deterministic component (line–of–sight or reflected) is present in the received signal in addition to the random multipath components. The amplitude $\sqrt{2}a_c$ of the received signal is modeled as a random variable with probability density function (pdf) given by [5]

$$f_{A_c}(a_c) = \frac{a_c}{\sigma^2} \exp\left(-\frac{a_c^2 + \alpha^2}{2\sigma^2}\right) I_0\left(\frac{\alpha a_c}{\sigma^2}\right) u(a_c) \tag{2.1}$$

where

$E(a_c^2) = \overline{a_c^2} = \alpha^2 + 2\sigma^2$ is the average received signal power,

$2\sigma^2$ is the power of the multipath component of the signal,

α^2 is the power of the deterministic component,

$I_0(\bullet)$ is the modified Bessel function of the first kind of order zero, and

$u(a_c)$ is the unit step function.

In order to quantitatively describe the power in the deterministic component relative to the power in the multipath component, the Ricean $\zeta - factor$ is defined [5, 12] as the ratio of the power in the deterministic component to the power in the multipath component. When $\zeta \to \infty$, (2.1) approaches a Gaussian pdf (deterministic component only), while, when $\zeta \to 0$, (2.1) approaches the Rayleigh distribution (multipath component only).

After some manipulations, (2.1) can be written in terms of the average received signal power and the $\zeta - factor$ as

$$f_{A_c}(a_c) = \frac{(\zeta+1)a_c}{\overline{a_c^2}} \exp\left(-\frac{(\zeta+1)a_c^2 + \zeta\overline{a_c^2}}{\overline{a_c^2}}\right) I_0\left(2\sqrt{\frac{\zeta}{s(\zeta+1)}}a_c\right) u(a_c). \qquad (2.2)$$

Figure 1 is a plot of Equation (2.2) for various values of ζ and for $s = 1$.

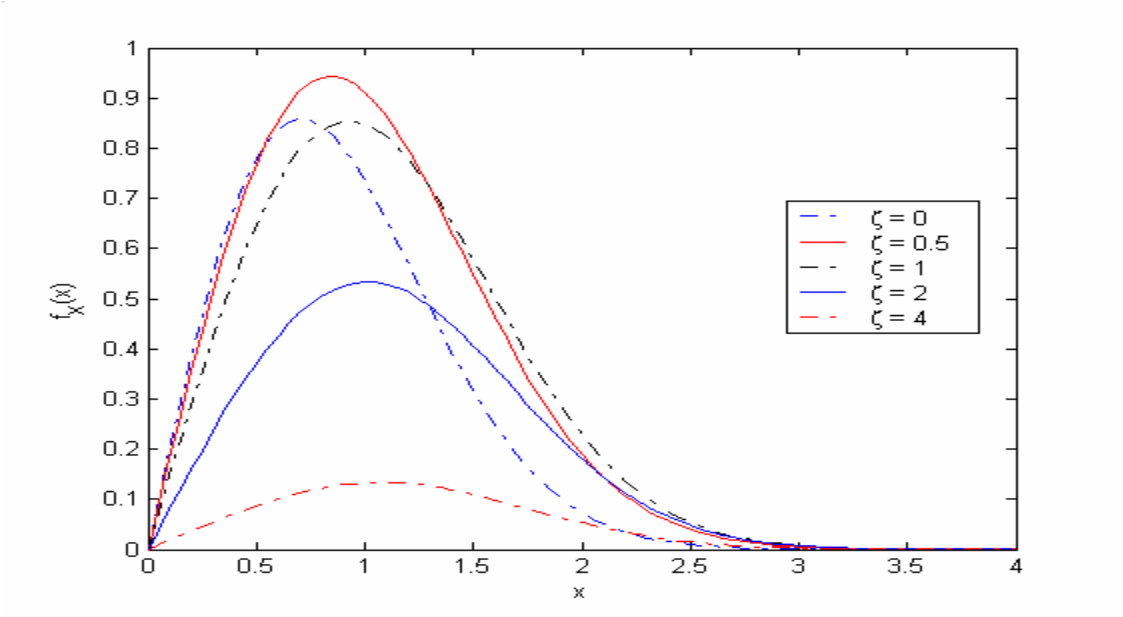

Figure 1. Ricean probability density function.

C. WAVEFORM PROPERTIES

1. Modulation Types

The *IEEE 802.11a* standard specifies an orthogonal frequency-division multiplexing (OFDM) system with BPSK, QPSK, 16–QAM and 64–QAM used for the modulation of the sub–carriers. These modulation techniques offer bandwidth efficiency along with ease of implementation. Figure 2 shows the constellation mapping for the sub–carrier modulation techniques [6].

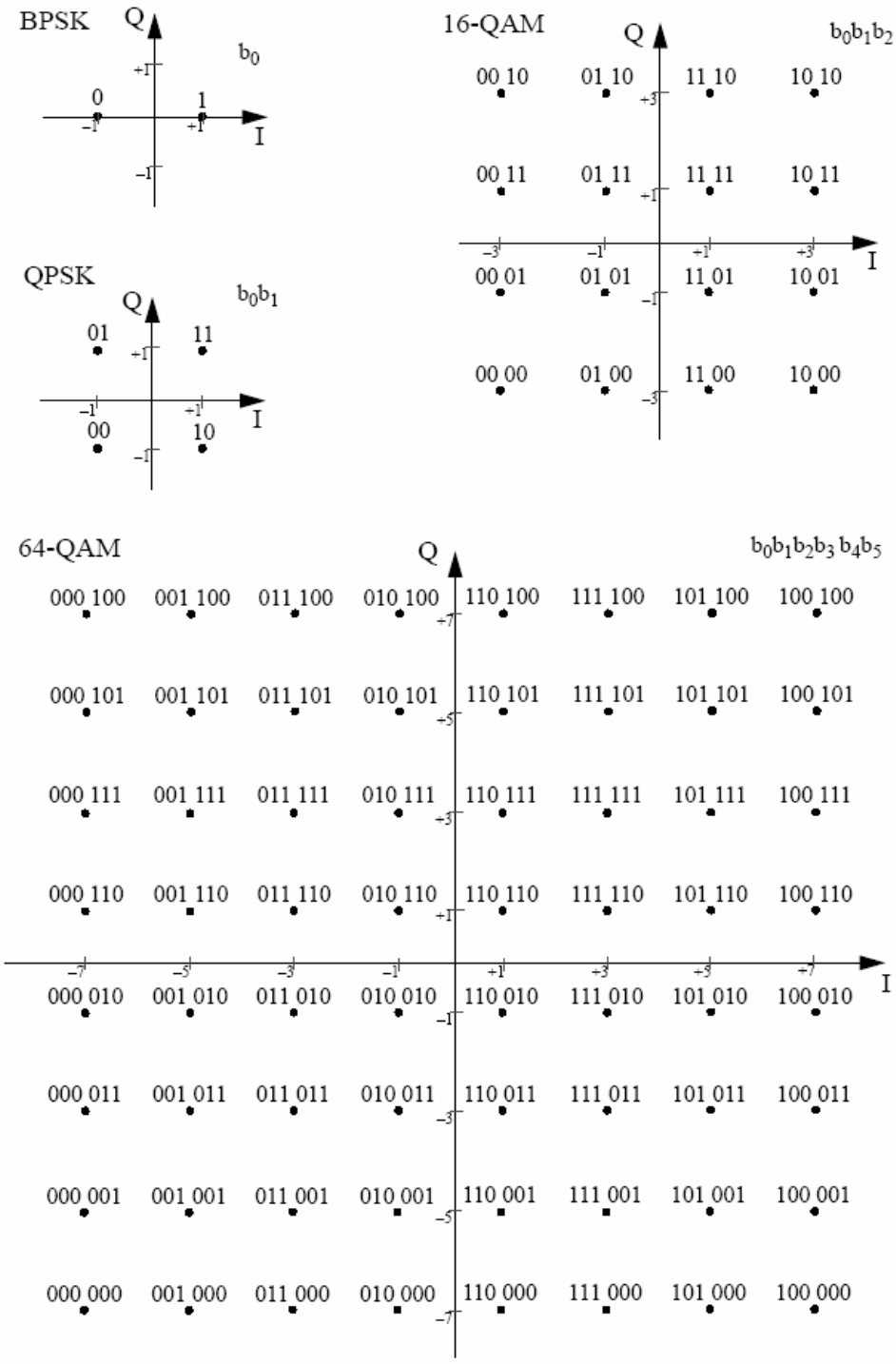

Figure 2. BPSK, QPSK, 16–QAM and 64–QAM constellation bit encoding [From Ref. 6.].

2. Forward Error Correction (FEC)

In order to reduce the effect of multipath channels on the system's performance, forward error correction coding is employed. The original bit stream is used to create an encoded bit stream which allows correction of errors to an extent depending on the code used. The *IEEE 802.11a* standard specifies that data are encoded with a convolutional encoder of coding rate $r = 1/2$ and constraint length $v = 7$ that uses the industry-standard generator polynomials $g_0 = 133_8$ and $g_1 = 171_8$ [6] (Figure 3).

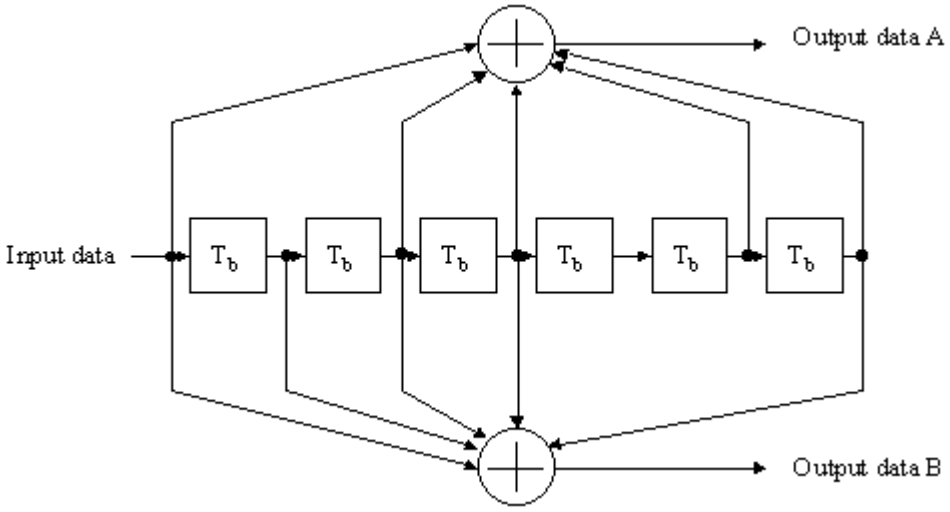

Figure 3. Convolutional encoder with $v = 7$ [From Ref. 6.].

Higher code rates ($r = 2/3$ and $r = 3/4$) are achieved by "puncturing" the $r = 1/2$ code, i.e., by omitting some of the encoded bits in the transmitter (thus, increasing the coding rate) and inserting a dummy zero metric in their place on the receiver side. Table 1 shows the combinations of data rates, modulation types and coding rates specified by the *IEEE 802.11a* standard.

Table 1. Rate Dependent Parameters [From Ref. 6.].

Data rate (Mbits/s)	Modulation	Code rate
6	BPSK	1/2
9	BPSK	3/4
12	QPSK	1/2
18	QPSK	3/4
24	16–QAM	1/2
36	16–QAM	3/4
48	64–QAM	2/3
54	64–QAM	3/4

D. SUMMARY

In this chapter we presented the Ricean fading model that describes the fading channel examined in this thesis. We also presented the sub–carrier waveforms and the forward error correction coding schemes specified by the *IEEE 802.11a* LAN standard. In the next chapter, we will examine the performance of these waveforms and coding schemes when the signal is transmitted over a Ricean fading channel with AWGN and pulsed–noise interference.

THIS PAGE INTENTIONALLY LEFT BLANK

III. PERFORMANCE FOR A RICEAN FADING CHANNEL WITH AWGN AND PULSED–NOISE INTERFERENCE

A. INTRODUCTION

This chapter describes the performance evaluation of the OFDM sub–carrier modulations implemented in the *IEEE 802.11a* standard when the signal is transmitted over a Ricean fading channel with additive white Gaussian noise (AWGN) and pulsed noise–like interference. Only the signal is assumed subject to fading. Both the non–coded and the coded cases with both hard decision decoding (HDD) and soft decision decoding (SDD) are examined, although the SDD analysis is limited to BPSK/QPSK due to the complexity of analyzing non–binary modulation combined with binary error correction codes.

B. WITHOUT FEC

1. BPSK/QPSK

The probability of bit error for BPSK/QPSK systems in AWGN and with no fading is given by

$$P_b = Q\left(\sqrt{\frac{2E_b}{N_0}}\right) \tag{3.1}$$

where $Q(\bullet)$ is the Q–function defined as

$$Q(z) = \frac{1}{\sqrt{2\pi}}\int_z^\infty \exp\left(\frac{-\lambda^2}{2}\right) d\lambda \tag{3.2}$$

and E_b/N_o is the per bit signal–to–noise ratio. Equivalently, (3.1) is given by [7]

$$P_b = Q\left(\sqrt{\frac{2a_c^2}{\sigma_0^2}}\right) \tag{3.3}$$

where σ_0^2 is the noise power and $\sqrt{2}a_c$ is the amplitude of the received signal.

In a Ricean fading channel, the received signal amplitude is modeled as a random variable having a Ricean probability density function, i.e., [5]

$$f_{A_c}(a_c) = \frac{a_c}{\sigma^2}\exp\left(-\frac{a_c^2+\alpha}{2\sigma^2}\right) I_0\left(\frac{\alpha a_c}{\sigma^2}\right) u(a_c), \tag{3.4}$$

where

$E\left(a_c^2\right) = \alpha^2 + 2\sigma^2$,

$2\sigma^2$ is the power of the multipath component of the signal,

α^2 is the power of the deterministic (line–of–sight or reflected) component, and

I_0 is the modified Bessel function of the first kind of zero order.

The probability in (3.3) is conditioned on the random variable a_c. Therefore, the probability of bit error when the signal is transmitted over a Ricean fading channel is the expected value of the conditioned probability in (3.3) over all potential values of a_c, i.e.,

$$P_b = \int_0^\infty P_b\left(a_c\right) f_{A_c}\left(a_c\right) da_c. \tag{3.5}$$

In [4], it is shown that the probability in (3.5) is

$$P_b \approx \frac{1}{2\sqrt{\pi\left(1.2 + 0.1\zeta\right)}} \frac{\zeta + 1}{\overline{\gamma}_b + \zeta + 1} \exp\left(-\frac{\zeta \overline{\gamma}_b}{\overline{\gamma}_b + \zeta + 1}\right) \tag{3.6}$$

where

$$\overline{\gamma}_b = \frac{\alpha^2 + 2\sigma^2}{\sigma_0^2} \tag{3.7}$$

is the average per bit signal–to–noise power ratio and

$$\zeta = \frac{\alpha^2}{2\sigma^2} \tag{3.8}$$

is the ratio of deterministic–to–multipath signal power.

In the presence of interference, the noise power is the sum of the AWGN and the interference power since the AWGN and the interference noise are modeled as independent random processes. Hence,

$$\overline{\gamma}_b = \frac{\alpha^2 + 2\sigma^2}{\sigma_0^2 + \sigma_I^2}. \tag{3.9}$$

We make the assumption that the average interference power is constant, regardless of the interference pulse duration determined by the interference duty cycle coefficient p ($0 < p \le 1$). Then, when interference is present

$$\overline{\gamma}_b = \frac{\alpha^2 + 2\sigma^2}{\sigma_0^2 + \frac{\sigma_I^2}{p}} = \frac{1}{\frac{\sigma_0^2 + \frac{\sigma_0^2}{p}}{\alpha^2 + 2\sigma^2}}. \tag{3.10}$$

By defining

$$\text{SNR} = \frac{\alpha^2 + 2\sigma^2}{\sigma_0^2}, \tag{3.11}$$

and

$$\text{SIR} = \frac{\alpha^2 + 2\sigma^2}{\sigma_I^2}, \tag{3.12}$$

then, when pulsed interference is present along with AWGN, we can express (3.10) as

$$\text{SNIR} = \overline{\gamma}_b = \frac{1}{\frac{1}{\text{SNR}} + \frac{1}{p\,\text{SIR}}}. \tag{3.13}$$

The pulsed interference may or may not affect a particular transmitted symbol with probability p or $(1-p)$, respectively. As a result,

$$\begin{aligned} P_b = {} & \Pr(\text{interference and AWGN}) \cdot P_b(\text{interference and AWGN}) \\ & + \Pr(\text{AWGN}) \cdot P_b(\text{AWGN}) \end{aligned} \tag{3.14}$$

where $\Pr(\text{interference and AWGN}) = p$ and $P_b(\text{interference and AWGN})$, $P_b(\text{AWGN})$ are computed from (3.6) by setting $\overline{\gamma}_b = \text{SNIR}$ and $\overline{\gamma}_b = \text{SNR}$, respectively.

The probability of bit error vs. SIR for BPSK/QPSK transmitted over a Ricean fading channel with AWGN and pulsed noise–like interference is plotted in Figure 4 for various values of the parameter ζ and for $p = 0.5$. The SNR is 32 dB, which, in the absence of interference, yields a probability of bit error on the order of 10^{-4} for $\zeta = 1$. As expected, performance improves as ζ increases, i.e., as the signal experiences less fading.

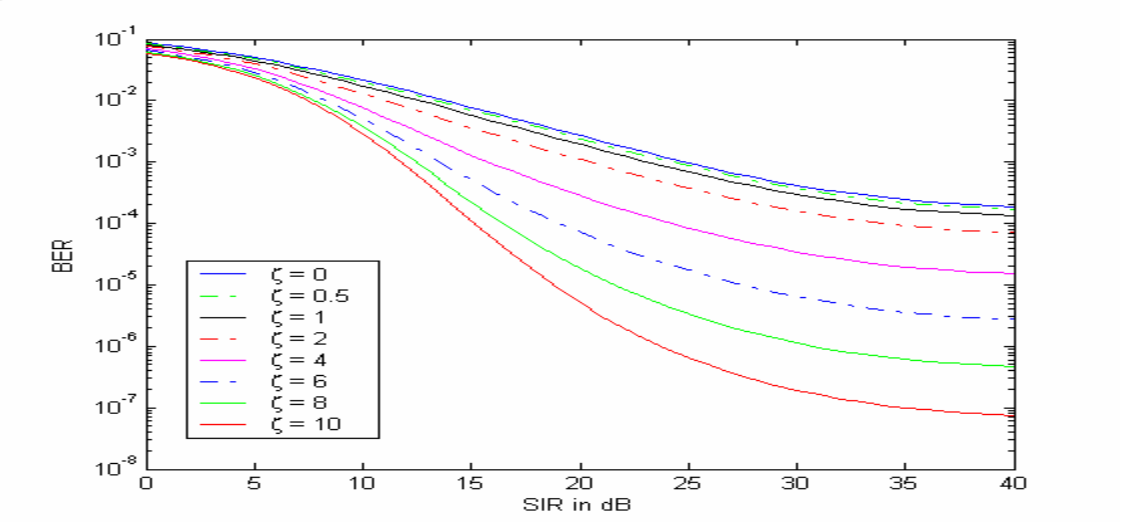

Figure 4. BPSK/QPSK in Ricean channel with AWGN and pulsed–noise interference $(p = 0.5)$.

In Figure 5, the probability of bit error vs. SIR is plotted for $\zeta = 1$ and $\zeta = 10$ and various values of p $(\text{SNR} = 32 \text{ dB})$. For strong fading $(\zeta = 1)$, the variation of the interference duty cycle, p, does not have an effect on P_b for $\text{SIR} > 15$ dB. Furthermore, while for $\zeta = 1$ the worst performance occurs for $p = 1$ (continuous interference), when $\zeta = 10$ (milder fading) and $\text{SIR} > 5$ dB, the worst performance occurs for small values of the interference duty cycle $(p = 0.1)$.

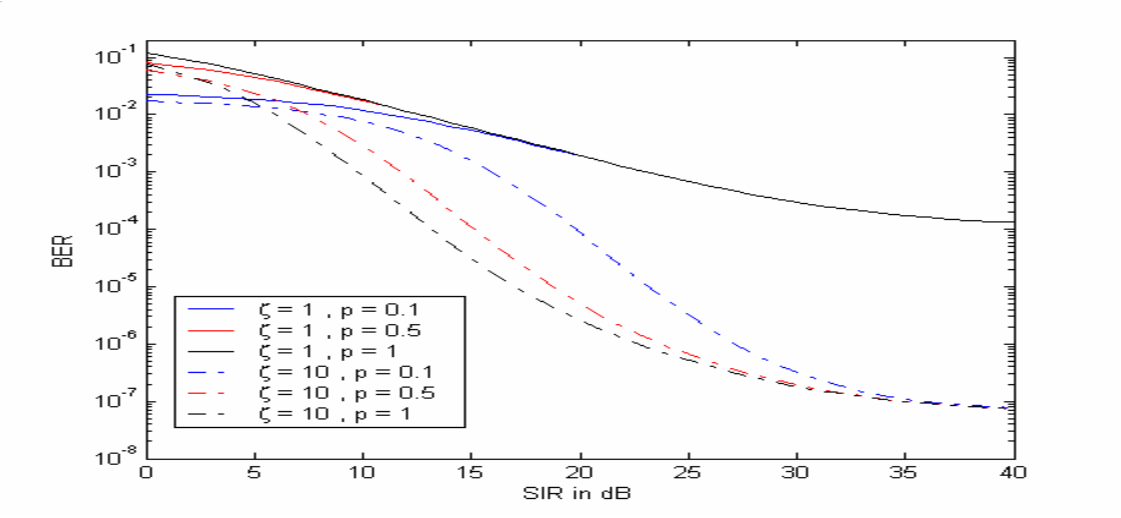

Figure 5. BPSK/QPSK in a Ricean channel with AWGN and pulsed–noise interference.

2. M–QAM

The probability of bit error for M–QAM systems with a square constellation is given [5] by

$$P_b = \frac{4\left(1-\frac{1}{\sqrt{M}}\right)}{q} Q\left(\sqrt{\frac{3q}{M-1}\frac{E_b}{N_0}}\right)\left[1-\left(1-\frac{1}{\sqrt{M}}\right)Q\left(\sqrt{\frac{3q}{M-1}\frac{E_b}{N_0}}\right)\right] \tag{3.15}$$

where

$M = 2^q$ is the size of the constellation,

q is the number of bits per symbol, and

$E_b/N_0 = a_c^2/\sigma_0^2$ is the per bit signal–to–noise power ratio.

In a Ricean fading channel, (3.15) is conditioned on the random variable a_c, with the probability density function given by (3.4). Then, the probability of bit error is the expected value of (3.15) over all potential values of a_c. In [4], it was shown that this probability is

$$P_b \approx \frac{4\left(1-\frac{1}{\sqrt{M}}\right)\exp\left(-\zeta\frac{3q\overline{\gamma}_b}{3q\overline{\gamma}_b+2(M-1)(\zeta+1)}\right)}{q\sqrt{2\pi c_2}\frac{3q\overline{\gamma}_b+2(M-1)(\zeta+1)}{2(M-1)(\zeta+1)}} - \frac{2\left(1-\frac{1}{\sqrt{M}}\right)^2\exp\left(-\zeta\frac{3q\overline{\gamma}_b}{3q\overline{\gamma}_b+2(M-1)(\zeta+1)}\right)}{\pi c_2 q\frac{3q\overline{\gamma}_b+(M-1)(\zeta+1)}{(M-1)(\zeta+1)}} \tag{3.16}$$

where $\overline{\gamma}_b$ is the average per bit signal–to–noise power ratio given by (3.7) and $c_2 = 2.6 + 0.1\zeta$.

To obtain the probability of bit error in the presence of pulsed–noise interference, it is again necessary to consider the two (distinct) events of symbol–with–interference and symbol–without–interference as represented by (3.14).

a. 16–QAM

The probability of bit error vs. SIR for 16–QAM transmitted over a Ricean fading channel with AWGN and pulsed noise–like interference is plotted in Figure 6 for various values of the parameter ζ and for $p = 0.5$. The SNR is 34 dB, which, in the absence of interference, yields a probability of bit error on the order of 10^{-4} for $\zeta = 1$. In Figure 7, the probability of bit error is plotted against SIR for $\zeta = 1$ and $\zeta = 10$ and for various values of p $(\text{SNR} = 34 \text{ dB})$.

As with BPSK/QPSK, there is improvement in performance when ζ increases, although improvement is not significant for $\text{SIR} < 10$ dB. For $\zeta = 1$, there is no effect on P_b when p is varied and $\text{SIR} > 20$ dB. At higher values of ζ and for $\text{SIR} > 10$ dB, it is the small values of p that represent the worst case from the P_b point of view.

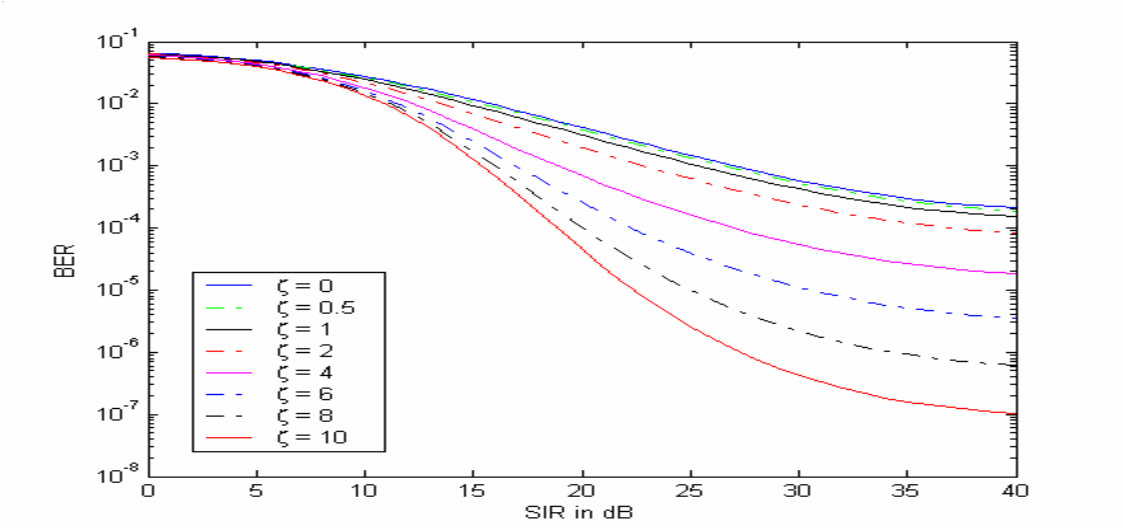

Figure 6. 16–QAM in Ricean channel with AWGN and pulsed–noise interference $(p = 0.5)$.

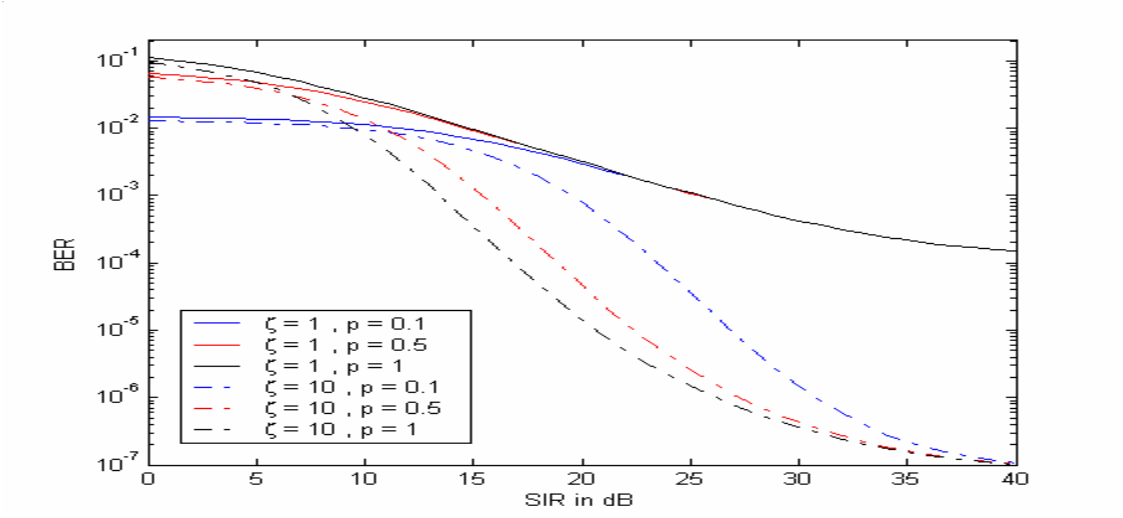

Figure 7. 16–QAM in Ricean channel with AWGN and pulsed–noise interference.

b. 64–QAM

The probability of bit error vs. SIR for 64–QAM transmitted over a Ricean fading channel with AWGN and pulsed noise–like interference is plotted in Figure 8 for various values of the parameter ζ and for $p = 0.5$. The SNR is 38 dB, which, in the absence of interference, yields a probability of bit error on the order of 10^{-4} for $\zeta = 1$. In Figure 9, the probability of bit error vs. SIR is plotted for various values of p and for $\zeta = 1,\ \zeta = 10\ (\text{SNR} = 38\ \text{dB})$.

As with BPSK/QPSK and 16–QAM, the performance improves when ζ increases and $\text{SIR} > 13$ dB. At higher values of ζ and for $\text{SIR} > 15$ dB, small values of p represent the worst case with respect to P_b. Variations of p have no effect on P_b for low values of ζ (strong fading) and $\text{SIR} > 23$ dB.

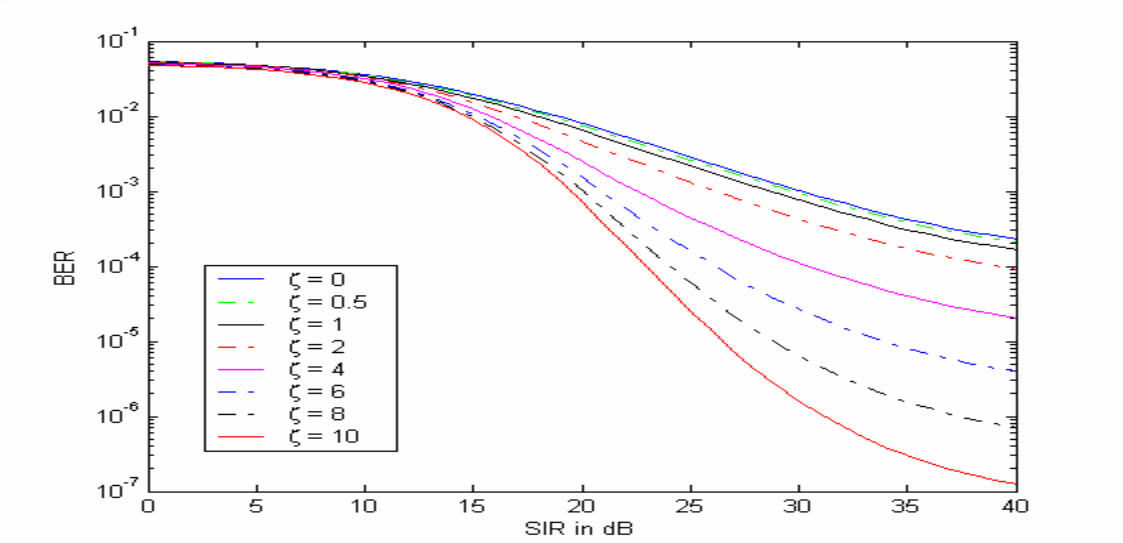

Figure 8. 64–QAM in Ricean channel with AWGN and pulsed–noise interference $(p = 0.5)$.

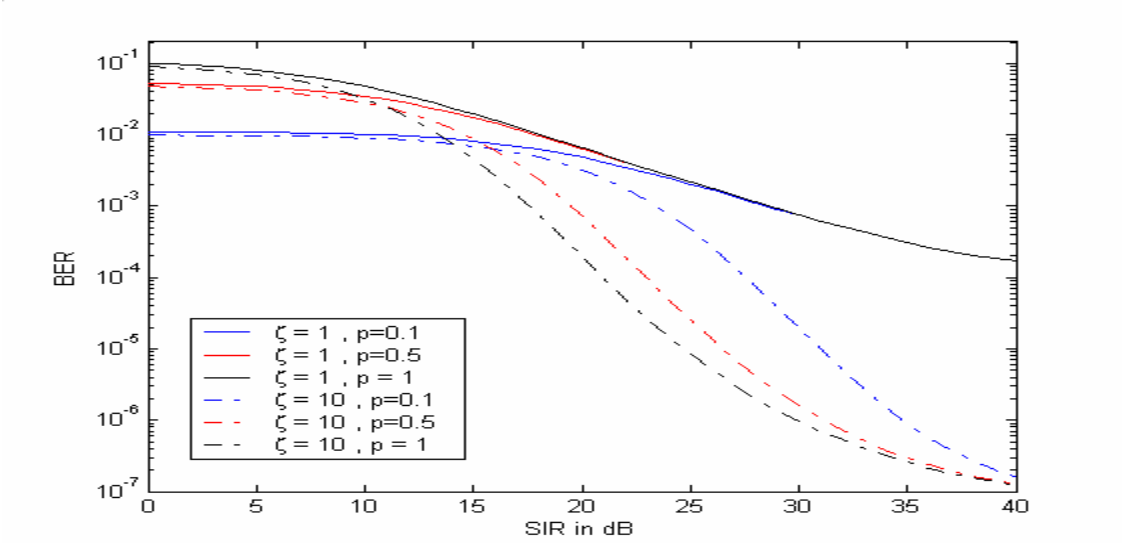

Figure 9. 64–QAM in Ricean channel with AWGN and pulsed–noise interference

C. WITH CONVOLUTIONAL CODING AND HARD DECISION DECODING (HDD)

The probability of bit error with convolutional coding is upper–bounded by [8]

$$P_b < \frac{1}{k} \sum_{d=d_{free}}^{\infty} B_d P_d \tag{3.17}$$

where

k is the number of data bits used to encode n channel bits,

d_{free} is the free distance of the code,

B_d are coefficients that depend on the code and represent the sum of all possible bit errors that can occur when the all–zero sequence is transmitted and a path of weight d is selected by the decoder, and

P_d is the probability of selecting a code sequence that differs from the correct sequence in d bits .

The first five terms of the sum in (3.17) dominate this upper bound.

If d is odd, the all–zero path will be correctly selected if the number of errors in the received sequence is less than $(d+1)/2;$ otherwise, the incorrect path will be selected. If d is even, the incorrect path is selected if the number of errors exceeds $d/2;$ while, if the number of errors equals $d/2$, then one of the paths has to be selected randomly. Therefore, for HDD and d odd

$$P_d = \sum_{k=\frac{d+1}{2}}^{d} \binom{d}{k} p_e^k (1-p_e)^{d-k} \tag{3.18}$$

while for HDD and d even

$$P_d = \sum_{k=\frac{d}{2}+1}^{d} \binom{d}{k} p_e^k (1-p_e)^{d-k} + \frac{1}{2}\binom{d}{\frac{d}{2}} p_e^{\frac{d}{2}} (1-p_e)^{\frac{d}{2}} \tag{3.19}$$

where p_e is the probability of bit error for the channel. It depends on the type of modulation used.

The values of B_d used in this thesis are listed in Table 2. They constitute a combination of the values for the best (maximum free distance) $r = 1/2$, $r = 3/4$, and $r = 2/3$ codes of constraint length $v = 7$ from [9] and of the best (maximum free distance) $r = 3/4$, and $r = 2/3$ "punctured" best $r = 1/2$ codes from [8].

Table 2. Weight Structure of the Convolutional Codes.

Rate	d_{free}	$B_{d_{free}}$	$B_{d_{free}+1}$	$B_{d_{free}+2}$	$B_{d_{free}+3}$	$B_{d_{free}+4}$
1/2	10	36	0	211	0	1404
2/3	6	3	81	402	1487	6793
3/4	5	42	252	1903	11,995	72,115

1. BPSK/QPSK with Convolutional Coding and HDD

For BPSK/QPSK, the probability p_e of bit error for the channel is given by substituting (3.6) into (3.14), but, due to the introduction of redundant bits, the mean signal–to–noise power ratios in $P_b(\text{AWGN})$ and $P_b(\text{interference and AWGN})$ (SNR and SNIR, respectively) have to be multiplied by the code rate r.

As expected, the use of coding yielded significantly improved performance. Apart from that, as shown below, the same phenomena are observed as for the non–coded case. Specifically, performance improves as ζ increases and there is no effect of the variation of the interference duty cycle beyond some SIR value when fading is strong. Also, for milder fading (larger ζ values), the worst performance occurs for low values of p and $\text{SIR} > 9$ dB, approximately.

a. BPSK/QPSK with Convolutional Coding and HDD with r = 1/2

The probability of bit error vs. SIR for BPSK/QPSK with convolutional coding and HDD for $r = 1/2$ when the signal is transmitted over a Ricean fading channel with AWGN and pulsed noise–like interference is plotted in Figure 10 for various values of the channel parameter ζ and for $p = 0.5$. The SNR is 18 dB, which, in the absence of interference, yields a probability of bit error on the order of 10^{-7} for $\zeta = 1$ [4]. In Figure 11 the probability of bit error vs. SIR is plotted for various values of p and for $\zeta = 1$, $\zeta = 10$ $(\text{SNR} = 18 \text{ dB})$.

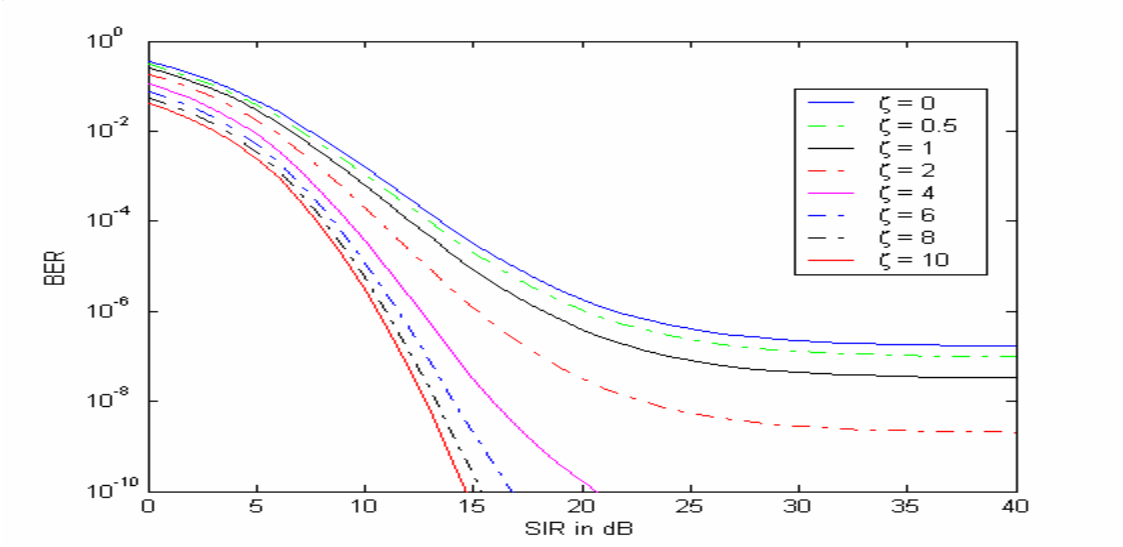

Figure 10. BPSK/QPSK with convolutional coding and HDD with $r = 1/2$ in a Ricean channel with AWGN and pulsed–noise interference $(p = 0.5)$.

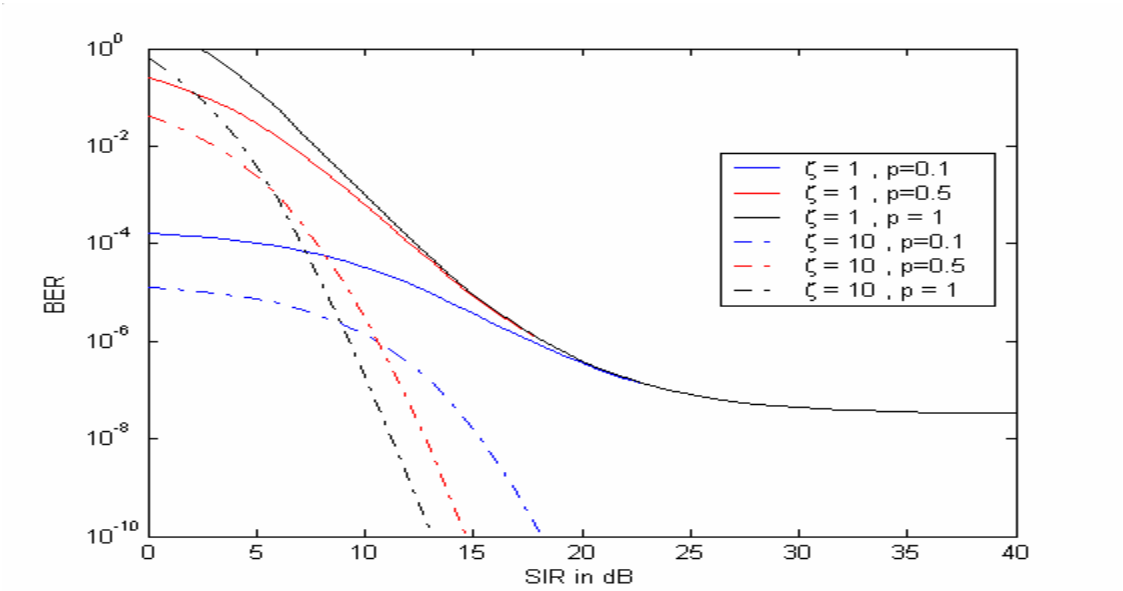

Figure 11. BPSK/QPSK with convolutional coding and HDD with $r = 1/2$ in a Ricean channel with AWGN and pulsed–noise interference.

b. BPSK/QPSK with Convolutional Coding and HDD with $r = 3/4$

The probability of bit error vs. SIR for BPSK/QPSK with convolutional coding with HDD and $r = 3/4$ when the signal is transmitted over a Ricean fading channel with AWGN and pulsed noise–like interference is plotted in Figure 12 for various

values of the parameter ζ and $p = 0.5$. The SNR is 28 dB, which, in the absence of interference, yields a probability of bit error on the order of 10^{-7} for $\zeta = 1$ [4]. In Figure 13 the probability of bit error vs. SIR is plotted for various values of p and for $\zeta = 1$, $\zeta = 10$ $(\text{SNR} = 28 \text{ dB})$.

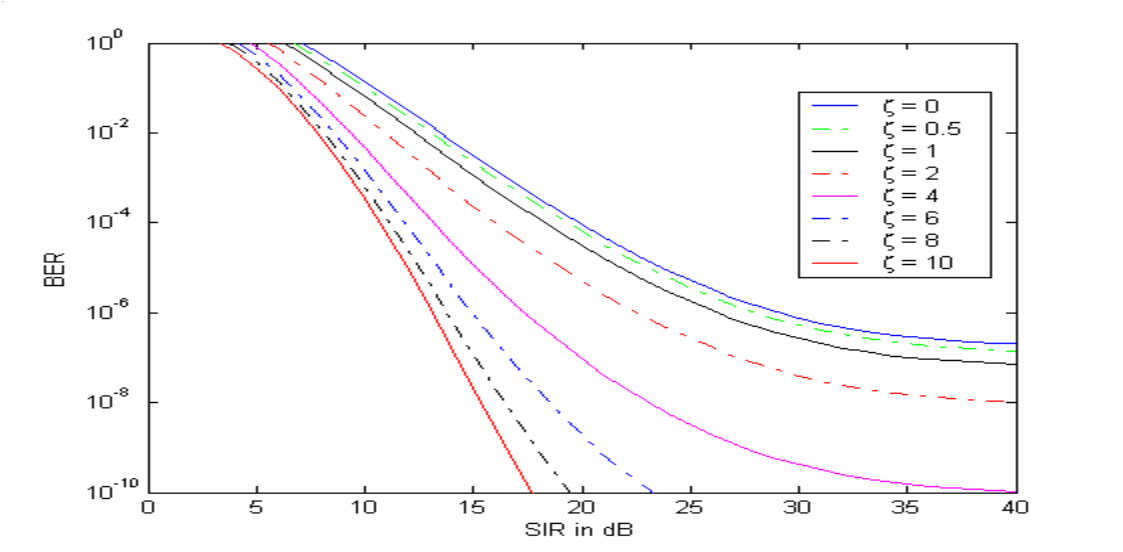

Figure 12. BPSK/QPSK with convolutional coding and HDD with $r = 3/4$ in a Ricean channel with AWGN and pulsed–noise interference $(p = 0.5)$.

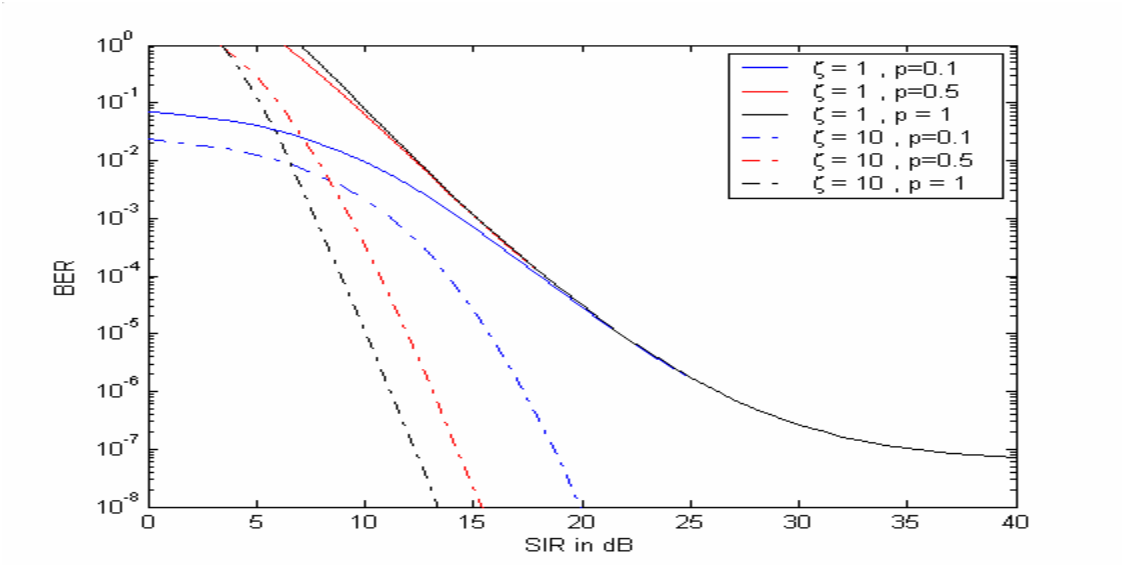

Figure 13. BPSK/QPSK with convolutional coding and HDD with $r = 3/4$ in a Ricean channel with AWGN and pulsed–noise interference.

2. M–QAM with Convolutional Coding and HDD

For M–QAM, the probability p of bit error for the channel is obtained by substituting (3.15) into (3.14). As with BPSK/QPSK, due to the introduction of redundant bits, the mean signal–to–noise power ratios in $P_b(\text{AWGN})$ and $P_b(\text{interference and AWGN})$ (SNR and SNIR, respectively) have to be multiplied by the code rate r.

The use of coding significantly improves performance. Otherwise, the same phenomena are observed as for the non–coded case (i.e., improvement in performance as ζ increases, no effect of the variation of the interference duty cycle beyond some SIR value when fading is strong, and worst performance occurring at low values of p when fading is less strong and $\text{SIR} > 15$ dB, approximately).

a. 16–QAM with Convolutional Coding and HDD with $r = 1/2$

The probability of bit error vs. SIR for 16–QAM with convolutional coding and HDD for $r = 1/2$ when the signal is transmitted over a Ricean fading channel with AWGN and pulsed noise–like interference is plotted in Figure 14 for various values of the parameter ζ and for $p = 0.5$. The SNR is 21 dB, which, in the absence of interference, yields a probability of bit error on the order of 10^{-7} for $\zeta = 1$ [4]. In Figure 15, the probability of bit error vs. SIR is plotted for various values of p and for $\zeta = 1$, $\zeta = 10$ $(\text{SNR} = 21 \text{ dB})$.

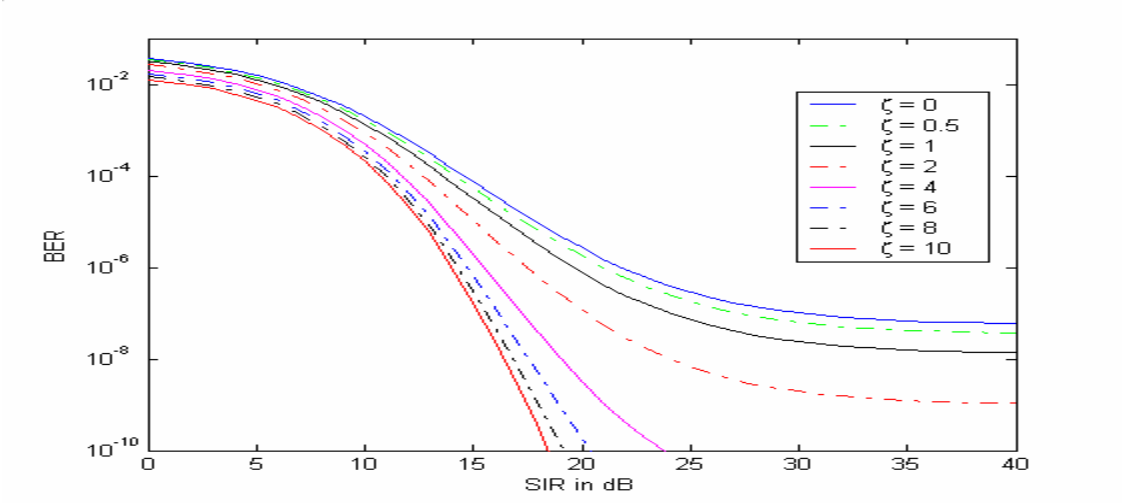

Figure 14. 16–QAM with convolutional coding and HDD with $r = 1/2$ in a Ricean channel with AWGN and pulsed–noise interference $(p = 0.5)$.

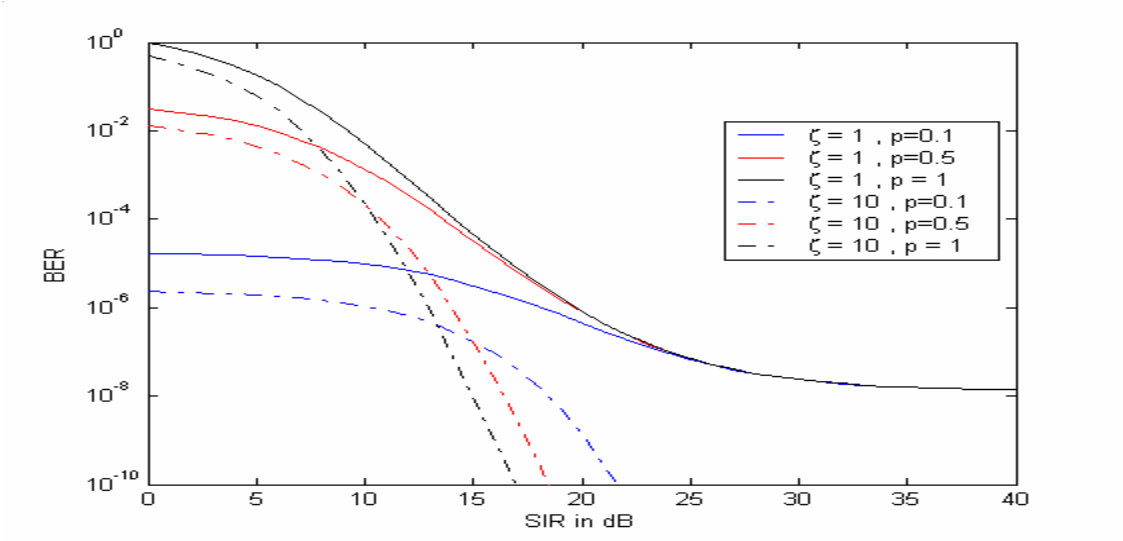

Figure 15. 16–QAM with convolutional coding and HDD with $r = 1/2$ in a Ricean channel with AWGN and pulsed–noise interference.

b. 16–QAM with Convolutional Coding and HDD with $r = 3/4$

The probability of bit error vs. SIR for 16–QAM with convolutional coding and HDD for $r = 3/4$ when the signal is transmitted over a Ricean fading channel with AWGN and pulsed noise–like interference is plotted in Figure 16 for various values of the parameter ζ and for $p = 0.5$. The SNR is 32 dB, which, in the absence of interference, yields a probability of bit error on the order of 10^{-7} for $\zeta = 1$ [4]. In Figure 17, the probability of bit error vs. SIR is plotted for various values of p and for $\zeta = 1$, $\zeta = 10$ $(\text{SNR} = 32 \text{ dB})$.

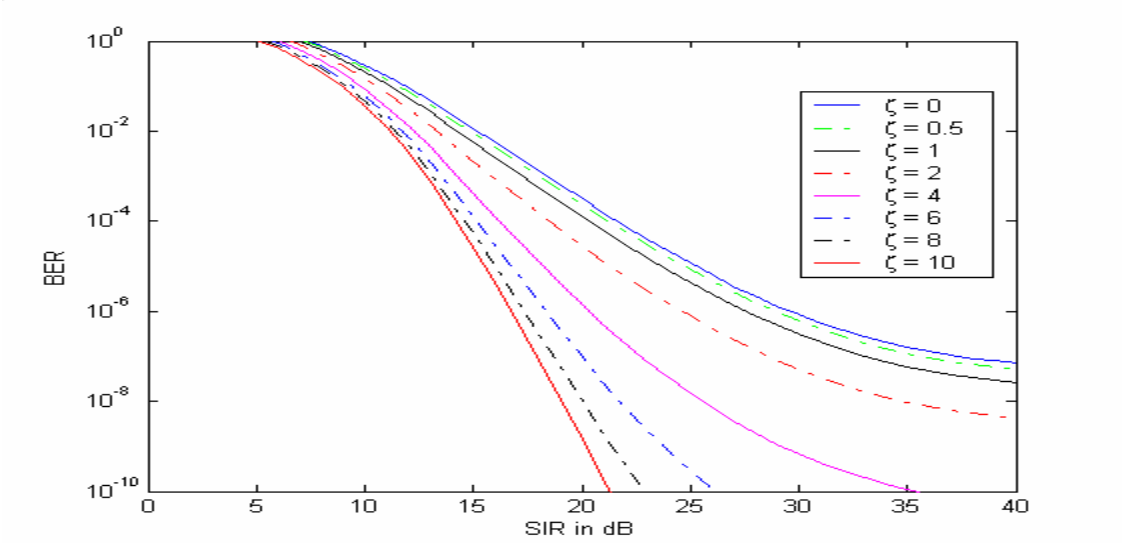

Figure 16. 16–QAM with convolutional coding and HDD with $r = 3/4$ in a Ricean channel with AWGN and pulsed–noise interference $(p = 0.5)$.

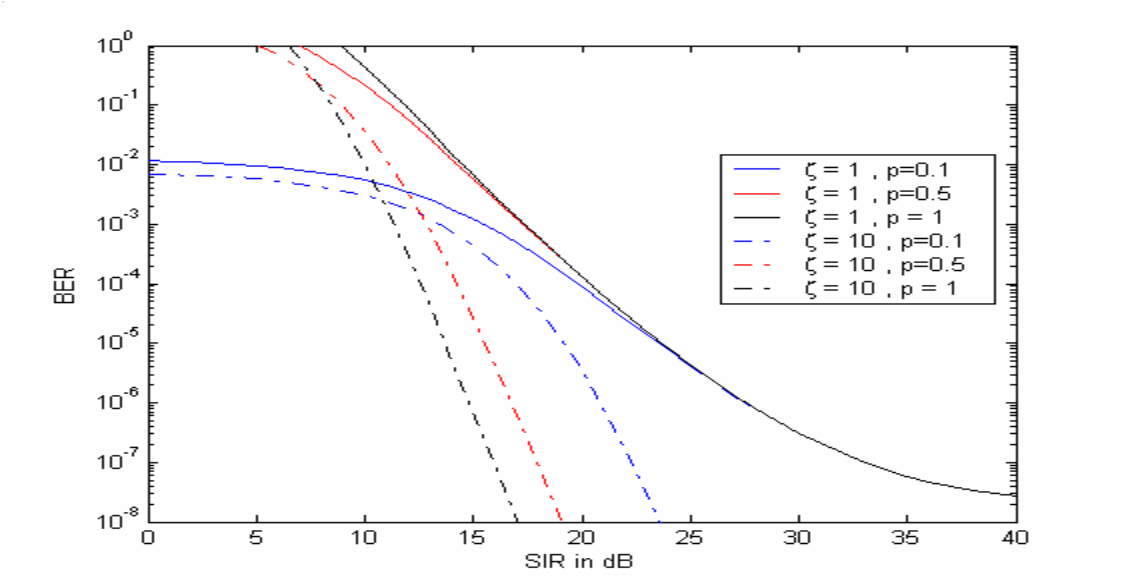

Figure 17. 16–QAM with convolutional coding and HDD with $r = 3/4$ in a Ricean channel with AWGN and pulsed–noise interference.

c. 64–QAM with Convolutional Coding and HDD with $r = 2/3$

The probability of bit error vs. SIR for 64–QAM with convolutional coding and HDD for $r = 2/3$ when the signal is transmitted over a Ricean fading channel with AWGN and pulsed noise–like interference is plotted in Figure 18 for various values of the channel parameter ζ and for $p = 0.5$. The SNR is 28 dB, which, in the absence of

interference, yields a probability of bit error on the order of 10^{-7} for $\zeta = 1$ [4]. In Figure 19, the probability of bit error vs. SIR is plotted for various values of p and $\zeta = 1$, $\zeta = 10$ $(\text{SNR} = 28 \text{ dB})$.

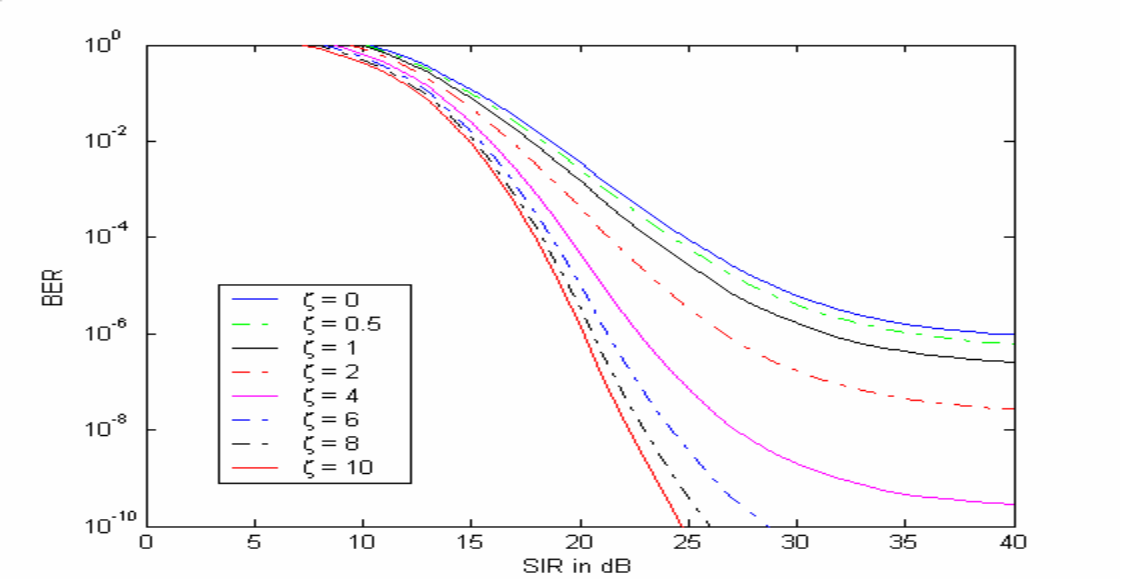

Figure 18. 64–QAM with convolutional coding and HDD with $r = 2/3$ in a Ricean channel with AWGN and pulsed–noise interference $(p = 0.5)$.

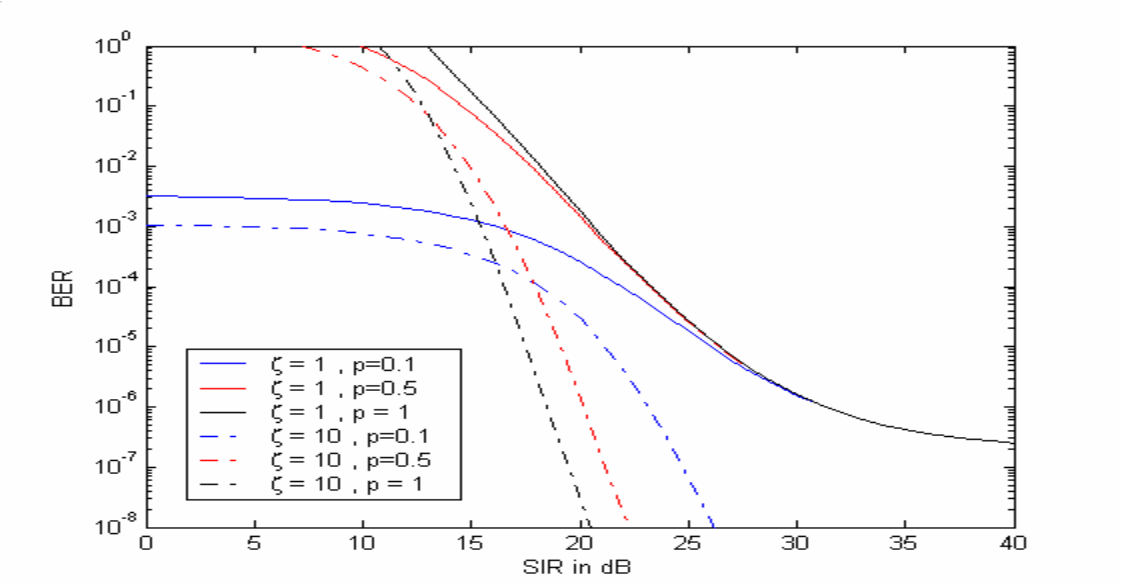

Figure 19. 64–QAM with convolutional coding and HDD with $r = 2/3$ in a Ricean channel with AWGN and pulsed–noise interference.

d. 64–QAM with Convolutional Coding and HDD with $r = 3/4$

The probability of bit error vs. SIR for 64–QAM with convolutional coding and HDD for $r = 3/4$ when the signal is transmitted over a Ricean fading channel with AWGN and pulsed noise–like interference is plotted in Figure 20 for various values of the channel parameter ζ and for $p = 0.5$. The SNR is 33 dB, which, in the absence of interference, yields a probability of bit error on the order of 10^{-7} for $\zeta = 1$ [4]. In Figure 21, the probability of bit error vs. SIR is plotted for various values of p and $\zeta = 1, \zeta = 10$ $(\text{SNR} = 33 \text{ dB})$.

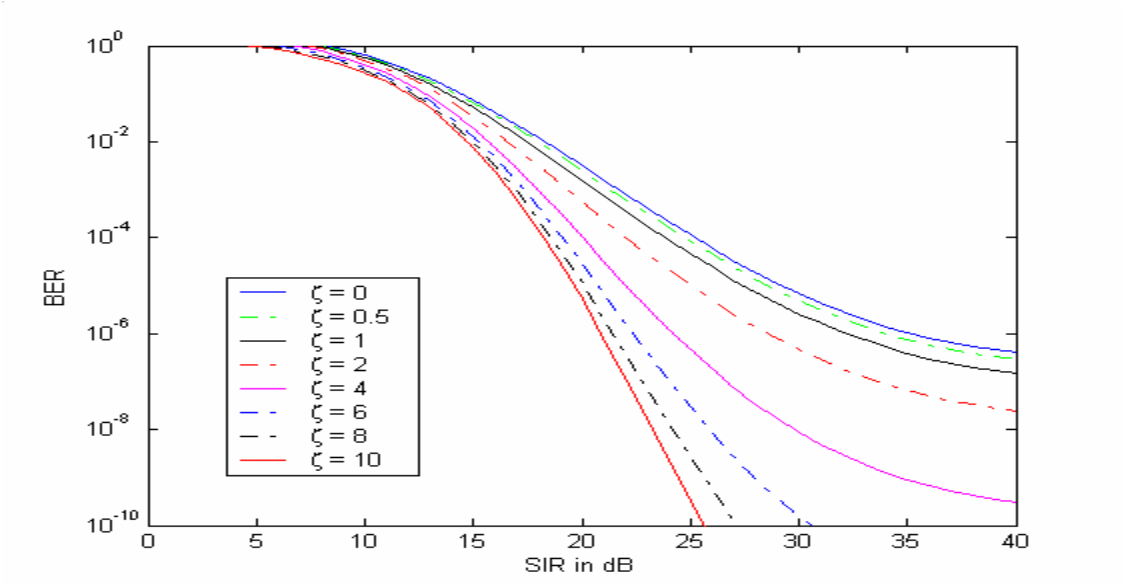

Figure 20. 64–QAM with convolutional coding and HDD with $r = 3/4$ in a Ricean channel with AWGN and pulsed–noise interference $(p = 0.5)$.

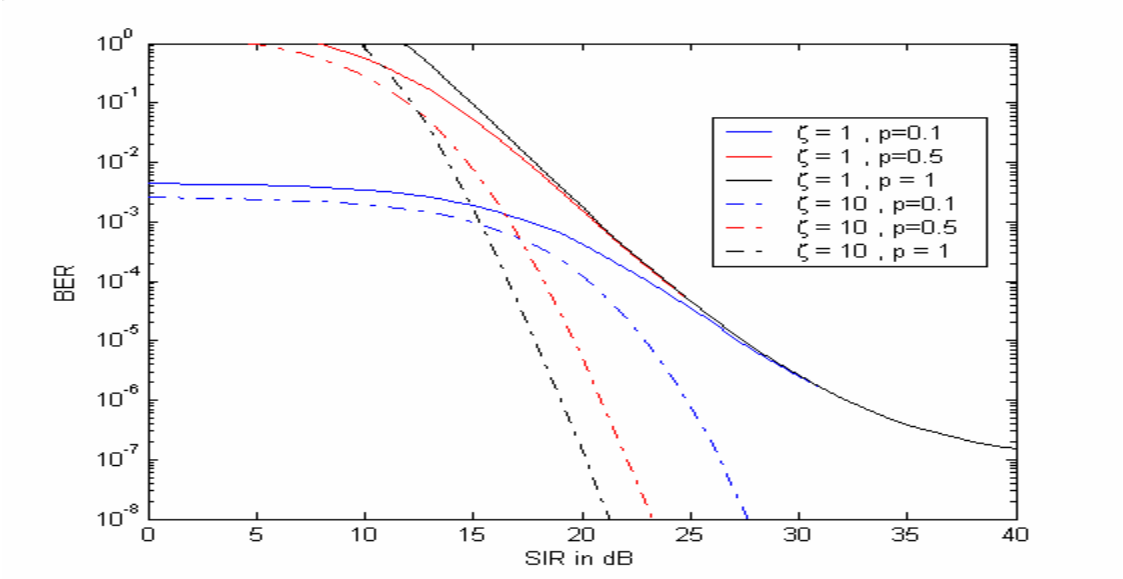

Figure 21. 64–QAM with convolutional coding and HDD with $r = 3/4$ in a Ricean channel with AWGN and pulsed–noise interference.

D. WITH CONVOLUTIONAL CODING AND SOFT DECISION DECODING (SDD)

For BPSK/QPSK with convolutional coding and soft decision decoding (SDD), (3.17) applies, but the probability P_d of selecting a path that differs from the correct path (by assumption, the all–zero path) in d bits is given by

$$P_d = \Pr\left(\sum_{l=1}^{d} \frac{a_{c_l} r_l}{\sigma_l^2} \geq 0 \right) \tag{3.20}$$

where

the index l runs over the set of the d bits,

a_{c_l} is the amplitude of the received signal (assumed to be a Ricean random variable) for the l^{th} bit,

r_l is the demodulator output for each of the d bits, and

σ_l^2 is the noise power for the l^{th} bit.

Equation (3.20) can be evaluated to yield

$$P_d = Q\left(\sqrt{2\left(\sum_{l=1}^{d}\frac{a_{c_l}^2}{\sigma_l^2}\right)}\right). \tag{3.21}$$

In the case of pulsed–noise interference with *i* of the *d* bits being affected by the interference, (3.21) can be written as

$$P_d = Q\left(\sqrt{2\left(\sum_{l=1}^{i}\frac{a_{c_l}^2}{\sigma_I^2}+\sum_{l=1}^{d\text{-}i}\frac{a_{c_l}^2}{\sigma_0^2}\right)}\right) \tag{3.22}$$

where the first sum corresponds to the *i* bits subject to the interference, σ_I^2 being the total noise power (AWGN plus interference) and the second sum corresponds to the *d–i* bits affected only by AWGN, σ_0^2 being the AWGN power. The probability P_d is conditional on a_{c_l}. In other words, it is necessary to find the expected value of (3.20) for all potential values of a_{c_l}. Equivalently, we can let

$$g = \sum_{l=1}^{i}\frac{a_{c_l}^2}{\sigma_I^2}+\sum_{l=1}^{d\text{-}i}\frac{a_{c_l}^2}{\sigma_0^2} \tag{3.23}$$

and calculate P_d as

$$P_d = \int_{-\infty}^{\infty} Q\left(\sqrt{2g}\right) f_G(g)\, dg \tag{3.24}$$

where $f_G(g)$ is the probability density function of the random variable *g*, which must be found.

In [4], it was shown that if a_{c_l} is a Ricean random variable, then the variable

$$h_1 = \sum_{l=1}^{i}\frac{a_{c_l}^2}{\sigma_I^2} \tag{3.25}$$

has a pdf given by

$$f_{H_1}(h_1) = \frac{h_1^{\frac{i-1}{2}}}{\left(\frac{i\alpha^2}{\sigma_I^2}\right)^{\frac{i-1}{2}}\frac{2\sigma^2}{\sigma_I^2}} \exp\left(\frac{-\left(h_1+\frac{i\alpha^2}{\sigma_I^2}\right)}{\frac{2\sigma^2}{\sigma_I^2}}\right) I_{i-1}\left(\frac{\frac{\alpha^2}{\sigma_I^2}\sqrt{ih_1}}{\frac{\sigma^2}{\sigma_I^2}}\right) u(h_1) \tag{3.26}$$

where $I_{i-1}(\bullet)$ is the modified Bessel function of order *i*–1. Similarly,

$$h_2 = \sum_{l=1}^{d-i} \frac{a_{cl}^2}{\sigma_0^2} \tag{3.27}$$

has a pdf given by

$$f_{H_2}(h_2) = \frac{h_2^{\frac{(d-i)-1}{2}}}{\left(\frac{(d-i)\alpha^2}{\sigma_0^2}\right)^{\frac{(d-i)-1}{2}} \frac{2\sigma^2}{\sigma_0^2}} \exp\left(\frac{-\left(h_2 + \frac{(d-i)\alpha^2}{\sigma_0^2}\right)}{\frac{2\sigma^2}{\sigma_0^2}}\right) \times I_{(d-i)-1}\left(\frac{\frac{\alpha^2}{\sigma_0^2}\sqrt{(d-i)h_2}}{\frac{\sigma^2}{\sigma_0^2}}\right) u(h_2). \tag{3.28}$$

Since *g* is the sum of h_1 and h_2, the probability density function of *g* is given by the convolution of the pdfs of h_1 and h_2. Furthermore, the Laplace transform of the pdf of *g* is equal to the product of the Laplace transforms of the pdfs of h_1 and h_2:

$$F_G(s) = L\left[f_G(g)\right] = L\left[f_{H_1}(h_1)\right] \cdot L\left[f_{H_2}(h_2)\right] \tag{3.29}$$

where $L[f]$ implies the Laplace transform of *f*.

The evaluation of the convolution of the two pdfs is an extremely complicated task. Therefore, the pdf of variable *g* was evaluated by making use of (3.29). The Laplace transform of the pdf of h_1 is defined as

$$F_{H_1}(s) = L\left[f_{H_1}(h_1)\right] = \int_0^\infty f_{H_1}(h_1) e^{-sh_1} dh_1 . \tag{3.30}$$

Substituting (3.26) into (3.30) and making use of the identity [5]

$$I_n(z) = (-j)^n J_n(jz) \tag{3.31}$$

where $J_n(\bullet)$ is the nth order Bessel function, we obtain

$$F_{H_1}(s)=\frac{\exp\left(\frac{-i\alpha^2}{2\sigma^2}\right)(-j)^{i-1}}{\left(\frac{i\alpha^2}{\sigma_I^2}\right)^{\frac{i-1}{2}}\frac{2\sigma^2}{\sigma_I^2}}\int_0^\infty h_1^{\frac{i-1}{2}}\exp\left(-\frac{h_1}{\frac{2\sigma^2}{\sigma_I^2}}-sh_1\right)J_{i-1}\left(\frac{j\frac{\alpha}{\sigma_I}\sqrt{ih_1}}{\frac{\sigma^2}{\sigma_I^2}}\right)dh_1. \quad (3.32)$$

In order to evaluate (3.32), we use the identity [10]

$$\int_0^\infty x^{m+\frac{n}{2}}e^{-vx}J_n\left(2\beta\sqrt{x}\right)dx=\frac{m!\beta^n e^{-\frac{\beta^2}{v}}}{v^{m+n+1}}L_m^n\left(\frac{\beta^2}{\nu}\right) \quad (3.33)$$

where $L_m^n(\bullet)$ is a Laguerre polynomial defined as

$$L_m^n\left(\frac{\beta^2}{\nu}\right)=\sum_{p=0}^{m}\frac{(-1)^p}{p!}\binom{m+n}{m-p}\left(\frac{\beta^2}{\nu}\right)^p. \quad (3.34)$$

For

$$m=0, \quad (3.35)$$

$$n=i-1, \quad (3.36)$$

$$v=\frac{1}{\frac{2\sigma^2}{\sigma_0^2}}+s, \quad (3.37)$$

and

$$2\beta=\frac{j\frac{\alpha}{\sigma_I}\sqrt{i}}{\frac{\sigma^2}{\sigma_I^2}}\Rightarrow\beta^2=\frac{(-1)\frac{\alpha^2}{\sigma_I^2}i}{\left(\frac{2\sigma^2}{\sigma_I^2}\right)^2}, \quad (3.38)$$

we get

$$L_0^{i-1}(\bullet)=1, \quad (3.39)$$

and

$$F_{H_1}(s)=\frac{\exp\left(\frac{-i\alpha^2}{2\sigma^2}\right)(-j)^{i-1}}{\left(\frac{i\alpha^2}{\sigma_I^2}\right)^{\frac{i-1}{2}}\frac{2\sigma^2}{\sigma_I^2}}\frac{\left(\frac{j\frac{\alpha}{\sigma_I}\sqrt{i}}{\frac{2\sigma^2}{\sigma_I^2}}\right)^{i-1}\exp\left(\frac{\frac{\alpha^2}{\sigma_I^2}i}{\left(\frac{2\sigma^2}{\sigma_I^2}\right)^2\left(s+\frac{1}{\frac{2\sigma^2}{\sigma_I^2}}\right)}\right)}{\left(s+\frac{1}{\frac{2\sigma^2}{\sigma_I^2}}\right)^i}. \tag{3.40}$$

After simplifications:

$$F_{H_1}(s)=\frac{\exp\left(\frac{-i\alpha^2}{2\sigma^2}\right)\exp\left(\frac{\frac{\alpha^2}{\sigma_I^2}i}{\left(\frac{2\sigma^2}{\sigma_I^2}\right)^2\left(s+\frac{1}{\frac{2\sigma^2}{\sigma_I^2}}\right)}\right)}{\left(\frac{2\sigma^2}{\sigma_I^2}\right)^i\left(s+\frac{1}{\frac{2\sigma^2}{\sigma_I^2}}\right)^i}. \tag{3.41}$$

By defining

$$\overline{h_1}=\frac{\overline{a_c^2}}{\sigma_I^2}=\frac{\alpha^2+2\sigma^2}{\sigma_I^2} \tag{3.42}$$

and since

$$\zeta=\frac{\alpha^2}{2\sigma^2}, \tag{3.43}$$

then

$$\frac{\alpha^2}{\sigma_I^2} = \frac{\zeta}{\zeta+1}\overline{h}_1 \,, \tag{3.44}$$

and

$$\frac{2\sigma^2}{\sigma_I^2} = \frac{\overline{h}_1}{\zeta+1}. \tag{3.45}$$

Substituting (3.43), (3.44), and (3.45) into (3.41), we get

$$F_{H_1}(s) = \frac{\exp(-i\zeta)\exp\left(\dfrac{\dfrac{\zeta}{\zeta+1}\overline{h}_1 i}{\left(\dfrac{\overline{h}_1}{\zeta+1}\right)^2\left(s+\dfrac{1}{\dfrac{\overline{h}_1}{\zeta+1}}\right)}\right)}{\left(\dfrac{\overline{h}_1}{\zeta+1}\right)^i\left(s+\dfrac{1}{\dfrac{\overline{h}_1}{\zeta+1}}\right)^i}. \tag{3.46}$$

Now, simplifying (3.46), we obtain

$$F_{H_1}(s) = \left(\frac{\exp(-\zeta)\exp\left(\dfrac{\zeta}{\dfrac{\overline{h}_1}{\zeta+1}s+1}\right)}{\dfrac{\overline{h}_1}{\zeta+1}s+1}\right)^i. \tag{3.47}$$

Similarly,

$$F_{H_2}(s)=\left(\frac{\exp(-\zeta)\exp\left(\frac{\zeta}{\frac{\overline{h_2}}{\zeta+1}s+1}\right)}{\frac{\overline{h_2}}{\zeta+1}s+1}\right)^{d-i} . \tag{3.48}$$

Therefore, from (3.47), (3.48), and (3.29),

$$F_G(s)=\left(\frac{\exp(-\zeta)\exp\left(\frac{\zeta}{\frac{\overline{h_1}}{\zeta+1}s+1}\right)}{\frac{\overline{h_1}}{\zeta+1}s+1}\right)^{i}\left(\frac{\exp(-\zeta)\exp\left(\frac{\zeta}{\frac{\overline{h_2}}{\zeta+1}s+1}\right)}{\frac{\overline{h_2}}{\zeta+1}s+1}\right)^{d-i} . \tag{3.49}$$

The inverse Laplace transform is

$$f_G(g)=L^{-1}\left[F_G(s)\right]=\frac{1}{2\pi j}\int_{c-j\infty}^{c+j\infty}F_G(s)e^{sg}\,ds \tag{3.50}$$

where c must be within the strip of convergence of $F_G(s)$. Since it is quite complicated to evaluate (3.50) analytically, we used the identity [5, 15]

$$\begin{aligned} f_X(x)=\frac{ce^{cx}}{\pi}\int_0^{\frac{\pi}{2}}\Big[\,&\mathrm{Re}\left\{F_X(c+jc\tan\varphi)\right\}\cos(cx\tan\varphi)\\ &-\mathrm{Im}\left\{F_X(c+jc\tan\varphi)\right\}\sin(cx\tan\varphi)\,\Big]\sec^2\varphi\;d\varphi \end{aligned} \tag{3.51}$$

to evaluate $f_G(g)$ numerically. In (3.51), c must be within the strip of convergence of $F_G(s)$ and is empirically selected.

With the above procedure, we can compute P_d conditioned on the number *i* of the bits subject to interference. Therefore, it is necessary to calculate the mean value of the conditioned $P_d(i)$ over all potential values of *i* (i.e., from zero to *d*). The probability that *i* out of *d* bits are affected by the interference is given by

$$P_I^d(i) = \binom{d}{i} p^i (1-p)^{d-i} \tag{3.52}$$

and the average P_d is given by

$$P_d = \sum_{i=0}^{d} P_I^d(i) P_d(i) = \sum_{i=0}^{d} \binom{d}{i} p^i (1-p)^{d-i} P_d(i) . \tag{3.53}$$

1. BPSK/QPSK with Convolutional Coding and SDD $r = 1/2$

The probability of bit error vs. SIR for BPSK/QPSK with convolutional coding and SDD for $r = 1/2$ when the signal is transmitted over a Ricean fading channel with AWGN and pulsed noise–like interference is plotted in Figure 22 for various values of the channel parameter ζ and for $p = 0.5$. The SNR is 10 dB, which, in the absence of interference, yields a probability of bit error in the order of 10^{-7} for $\zeta = 1$ [4]. In Figure 23, the probability of bit error vs. SIR is plotted for various values of *p* and for $\zeta = 1$, $\zeta = 10$ $(\text{SNR} = 10 \text{ dB})$.

The use of SDD eliminates the phenomenon of the worst performance occurring for low values of the interference duty cycle *p*. In Figure 20 we see that, within the P_b range of interest, continuous interference represents the worst–case scenario regardless of the degree of signal fading.

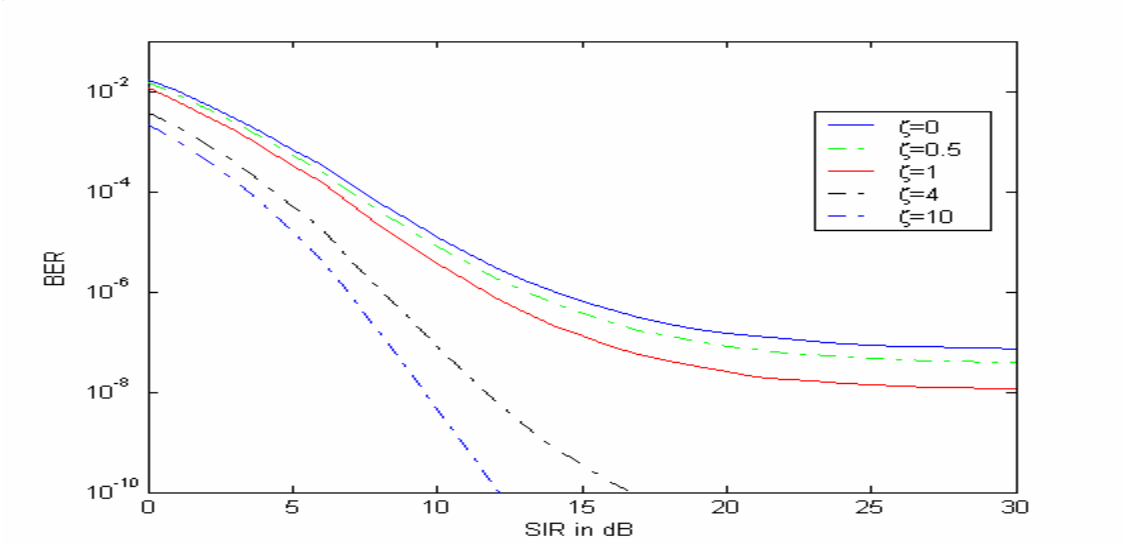

Figure 22. BPSK/QPSK with convolutional coding and SDD for $r = 1/2$ in a Ricean channel, with AWGN and pulsed–noise interference $(p = 0.5)$.

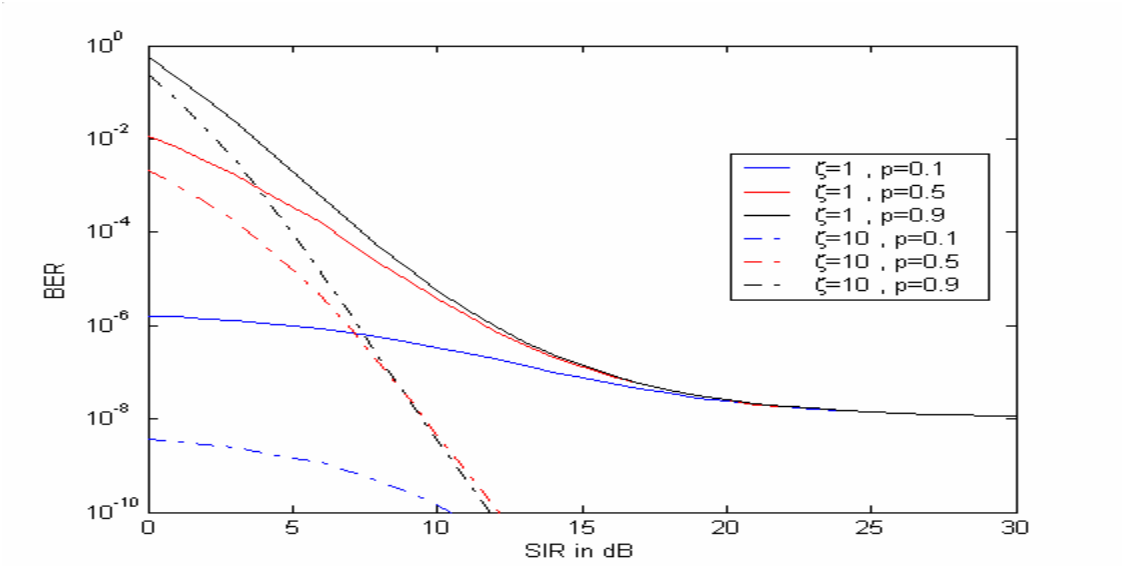

Figure 23. BPSK/QPSK with convolutional coding and SDD for $r = 1/2$ in a Ricean channel, with AWGN and pulsed–noise interference.

2. BPSK/QPSK with Convolutional Coding and SDD $r = 3/4$

The probability of bit error vs. SIR for BPSK/QPSK with convolutional coding and SDD for $r = 3/4$ when the signal is transmitted over a Ricean fading channel with AWGN and pulsed noise–like interference is plotted in Figure 24 for various values of the channel parameter ζ and for $p = 0.5$. The SNR is 15 dB, which, in the absence of in-

terference, yields a probability of bit error on the order of 10^{-7} for $\zeta = 1$ [4]. In Figure 25, the probability of bit error vs. SIR is plotted for various values of p and for $\zeta = 1$, $\zeta = 10$ $(\text{SNR} = 15 \text{ dB})$.

For mild fading and $\text{SIR} > 8$ dB, the worst performance occurs for low values of p but to an extent significantly reduced compared to the non–coded and the coded–with–HDD cases.

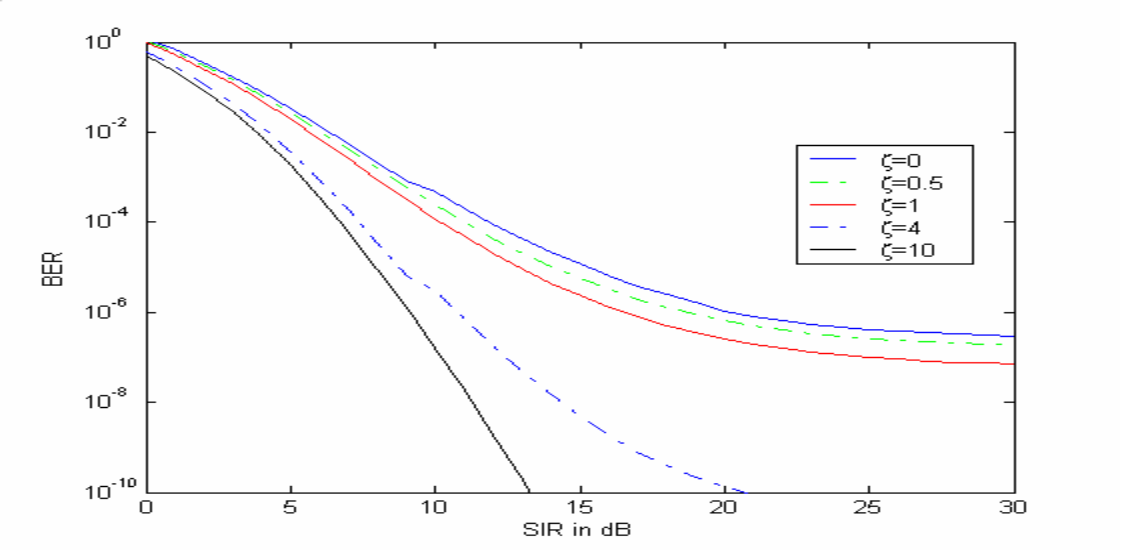

Figure 24. BPSK/QPSK with convolutional coding and SDD for $r = 3/4$ in a Ricean channel with AWGN and pulsed–noise interference $(p = 0.5)$.

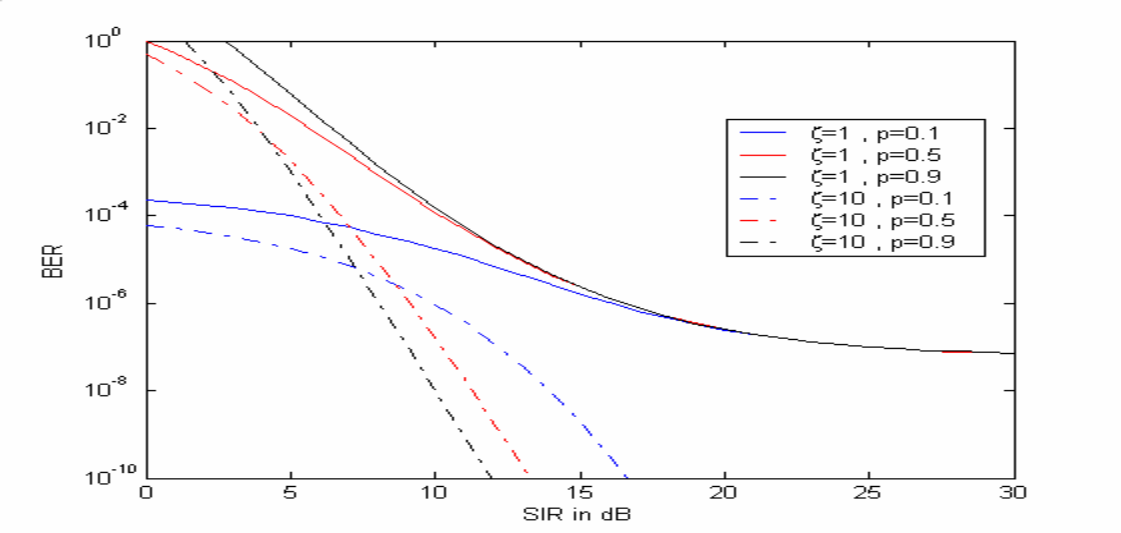

Figure 25. BPSK/QPSK with convolutional coding and SDD for $r = 3/4$ in a Ricean channel with AWGN and pulsed–noise interference.

E. SUMMARY

This chapter examined the effect of non–fading pulsed, noise–like interference and AWGN when the signal is transmitted over a Ricean fading channel. Results for the non–coded case and the coded–with–HDD case were obtained for all modulations specified in the *IEEE 802.11a* standard and for the coded–with–SDD case for BPSK/QPSK only. The effect on performance of the fading and the interference was evaluated in terms of the channel parameter ζ (degree of fading) and the pulsed interference duty cycle p.

In the next chapter, we examine the effect of pulsed, noise–like interference and AWGN when the signal is transmitted over a Ricean fading channel and the interference signal is also subject to fading.

IV. PERFORMANCE ANALYSIS FOR A RICEAN FADING CHANNEL WITH RICEAN FADING PULSED–NOISE INTERFERENCE

A. INTRODUCTION

The previous chapter examined receiver performance when a digital signal is transmitted over a Ricean fading channel with non–fading, noise–like pulsed interference and AWGN. The current chapter evaluates receiver performance when the interference signal also experiences Ricean fading. In this case, the received signal and the noise are modeled as random variables, and the probability of bit error is conditional on both. Due to the complexity of the analysis, however, the evaluation is limited to few special cases and, as far as the implementation of error correction coding is concerned, only hard decision decoding was examined.

B. THE GENERAL CASE

The probability of bit error for a BPSK/QPSK signal in AWGN with no channel fading is given by

$$P_b = Q\left(\sqrt{\frac{2a_c^2}{\sigma_N^2}}\right) \tag{4.1}$$

where a_c^2 represents the received signal power and σ_N^2 represents the noise power. In the presence of noise–like interference along with AWGN, σ_N^2 represents the combined AWGN and interference power, i.e., $\sigma_N^2 = \sigma_0^2 + \sigma_I^2$. In order to simplify the analysis, we assume that the AWGN power σ_0^2 is negligible compared to the interference power σ_I^2. In other words,

$$\sigma_N^2 \approx \sigma_I^2. \tag{4.2}$$

When the desired signal and the interfering signal both experience fading, a_c^2 and σ_I^2 are modeled as random variables, and (4.1) gives the probability of bit error conditioned on these two variables. The probability of bit error is also conditioned on these random variables when using M–QAM instead of BPSK/QPSK.

In order to obtain the unconditional probability of bit error, it is necessary to find the expected value of the conditional probability in (4.1) (or of the respective formula for M–QAM) over all possible values of a_c^2 and σ_I^2.

In the case of a signal subjected to Ricean fading, the probability density function of a_c is given by [5]

$$f_{A_c}\left(a_c\right) = \frac{a_c}{\sigma_s^2} \exp\left(-\frac{a_c^2 + \alpha_s^2}{2\sigma_s^2} \right) I_0\left(\frac{\alpha_s a_c}{\sigma_s^2} \right) \tag{4.3}$$

where

$E\left(a_c^2\right) = \alpha_s^2 + 2\sigma_s^2$,

$2\sigma_s^2$ is the power of the multipath component of the signal,

α_s^2 is the power of the deterministic component, and

I_0 is the modified Bessel function of the first kind of zero order.

Setting

$$s = a_c^2, \tag{4.4}$$

(should not be confused with the variable *s* of the Laplace transform in Chapter III) we get

$$a_c = \sqrt{s}, \tag{4.5}$$

and

$$\frac{ds}{da_c} = 2a_c. \tag{4.6}$$

From [11],

$$f_S\left(s\right) = \frac{1}{\left| ds \middle/ da_c \right|} f_{A_c}\left(a_c\right)\Bigg|_{a_c = \sqrt{s}} = \frac{1}{2a_c} \frac{a_c}{\sigma_s^2} \exp\left(-\frac{a_c^2 + \alpha_s^2}{2\sigma_s^2} \right) I_0\left(\frac{\alpha_s a_c}{\sigma_s^2} \right)\Bigg|_{a_c = \sqrt{s}}. \tag{4.7}$$

Therefore,

$$f_S(s) = \frac{1}{2\sigma_s^2} \exp\left(-\frac{s+\alpha_s^2}{2\sigma_s^2}\right) I_0\left(\frac{\alpha_s\sqrt{s}}{\sigma_s^2}\right). \tag{4.8}$$

Similarly, for the noise–like interference signal, we set

$$n = \sigma_I^2 \tag{4.9}$$

and obtain

$$f_N(n) = \frac{1}{2\sigma_n^2} \exp\left(-\frac{n+\alpha_n^2}{2\sigma_n^2}\right) I_0\left(\frac{\alpha_n\sqrt{n}}{\sigma_n^2}\right) \tag{4.10}$$

where

$E(n) = \alpha_n^2 + 2\sigma_n^2$,

$2\sigma_n^2$ is the power of the multipath component of the interference signal, and

α_n^2 is the power of the deterministic interference component.

By defining

$$z = \frac{s}{n}, \tag{4.11}$$

then, from (4.1), (4.4), and (4.9), the conditional probability of bit error for BPSK/QPSK is

$$P_b = Q\left(\sqrt{2z}\right) \tag{4.12}$$

and the unconditional probability is given by the mean value of (4.12), i.e.,

$$P_b = \int_{-\infty}^{\infty} Q\left(\sqrt{2z}\right) f_Z(z)\, dz \tag{4.13}$$

where $f_Z(z)$ is the probability density function of z and has to be evaluated. From [11]

$$f_Z(z) = \int_{-\infty}^{\infty} |n|\, f_S(zn)\, f_N(n)\, dn. \tag{4.14}$$

By substituting (4.7) and (4.10) into (4.14) and given that n assumes only positive values, we get

$$f_Z(z)=\int_0^\infty n\frac{1}{2\sigma_s^2}\exp\left(-\frac{zn+\alpha_s^2}{2\sigma_s^2}\right)I_0\left(\frac{\alpha_s\sqrt{zn}}{\sigma_s^2}\right)\frac{1}{2\sigma_n^2}\exp\left(-\frac{n+\alpha_n^2}{2\sigma_n^2}\right)I_0\left(\frac{\alpha_n\sqrt{n}}{\sigma_n^2}\right)dn. \quad (4.15)$$

From the identity

$$I_n(t)=(-j)^n J_n(jt) \quad (4.16)$$

we get

$$I_0(t)=J_0(jt), \quad (4.17)$$

and by substituting (4.17) into (4.15),

$$\begin{aligned} f_Z(z)=&\frac{1}{4\sigma_s^2\sigma_n^2}\exp\left(\frac{-\alpha_s^2}{2\sigma_s^2}+\frac{-\alpha_n^2}{2\sigma_n^2}\right)\\ &\times\int_0^\infty n\exp\left(\frac{-zn}{2\sigma_s^2}+\frac{-n}{2\sigma_n^2}\right)J_0\left(\frac{j\alpha_s\sqrt{zn}}{\sigma_s^2}\right)J_0\left(\frac{j\alpha_n\sqrt{n}}{\sigma_n^2}\right)dn. \end{aligned} \quad (4.18)$$

From [10], we know that

$$\begin{aligned} \int_0^\infty x^{\lambda+1}e^{-\alpha x^2}J_\mu(\beta x)J_\nu(\gamma x)\,dx=&\frac{\beta^\mu\gamma^\nu\alpha^{-\frac{\mu+\nu+\lambda+2}{2}}}{2^{\mu+\nu+1}\Gamma(\nu+1)}\\ &\times\sum_{m=0}^\infty\frac{\Gamma\left(m+\frac{1}{2}\nu+\frac{1}{2}\mu+\frac{1}{2}\lambda+1\right)}{m!\,\Gamma(m+\mu+1)}\left(-\frac{\beta^2}{4\alpha}\right)^m F\left(-m,-\mu-m;\nu+1;\frac{\gamma^2}{\beta^2}\right) \end{aligned} \quad (4.19)$$

where $F(\bullet)$ is the Gauss hypergeometric function, defined as

$$\begin{aligned} F(\alpha,\beta;\gamma;z)=&1+\frac{\alpha\beta}{\gamma}z+\frac{\alpha(\alpha+1)\beta(\beta+1)}{\gamma(\gamma+1)2}z^2\\ &+\frac{\alpha(\alpha+1)(\alpha+2)\beta(\beta+1)(\beta+2)}{\gamma(\gamma+1)(\gamma+2)2\,3}z^3+\ldots\ . \end{aligned} \quad (4.20)$$

The integral in (4.18) is similar to that in (4.19) if we let $\sqrt{n}=x,\ dn=2x\,dx,$

$\mu=0,\ \nu=0,\ \alpha=\frac{z}{2\sigma_s^2}+\frac{1}{2\sigma_n^2},\ \beta=j\frac{\alpha_s\sqrt{z}}{\sigma_s^2},\ \gamma=j\frac{\alpha_n}{\sigma_n^2},$ and $\lambda+1=3$ or $\lambda=2$. However, the resultant form is too complicated to analyze further. Therefore, some particular cases were examined.

C. PERFORMANCE ANALYSIS FOR A RAYLEIGH FADING SIGNAL WITH RICEAN FADING PULSED–NOISE INTERFERENCE

In the case of Rayleigh signal fading and Ricean interference fading, we set $\alpha_s = 0$ in (4.18) and obtain

$$f_Z(z) = \frac{1}{4\sigma_s^2\sigma_n^2}\exp\left(\frac{-\alpha_n^2}{2\sigma_n^2}\right)\int_0^\infty n\exp\left(-n\left(\frac{z}{2\sigma_s^2}+\frac{1}{2\sigma_n^2}\right)\right)J_0(0)\,J_0\left(\frac{j\alpha_n\sqrt{n}}{\sigma_n^2}\right)dn. \quad (4.21)$$

Using, again, the identity (3.31) with

$$m = 1, \quad (4.22)$$

$$n = 0, \quad (4.23)$$

$$v = \frac{z}{2\sigma_s^2}+\frac{1}{2\sigma_n^2} = \frac{z\sigma_n^2+\sigma_s^2}{2\sigma_s^2\sigma_n^2}, \quad (4.24)$$

and

$$2\beta = j\frac{\alpha_n}{\sigma_n^2} \Rightarrow \beta^2 = -\frac{\alpha_n^2}{4\sigma_n^2} \Rightarrow \frac{\beta^2}{v} = -\frac{\alpha_n^2\sigma_s^2}{2\sigma_n^2\left(z\sigma_n^2+\sigma_s^2\right)} \quad (4.25)$$

and given that [5]

$$L_1^k(x) = k+1-x \Rightarrow L_1^0\left(\frac{\beta^2}{v}\right) = 1-\frac{\beta^2}{v}, \quad (4.26)$$

then

$$f_Z(z) = \frac{\sigma_n^2\sigma_s^2}{\left(z\sigma_n^2+\sigma_s^2\right)^2}\exp\left(-\frac{\alpha_n^2}{2\sigma_n^2}\frac{z\sigma_n^2}{z\sigma_n^2+\sigma_s^2}\right)\left(1+\frac{\alpha_n^2}{2\sigma_n^2}\frac{\sigma_s^2}{z\sigma_n^2+\sigma_s^2}\right). \quad (4.27)$$

Since

$$\zeta_n = \frac{\alpha_n^2}{2\sigma_n^2} \quad (4.28)$$

$$\overline{s} = \overline{\alpha_c^2} = 2\sigma_s^2 \Rightarrow \sigma_s^2 = \frac{\overline{s}}{2}, \quad (4.29)$$

and

$$\overline{n} = \overline{\sigma_I^2} = \alpha_n^2+\sigma_n^2 = 2\sigma_n^2\left(\zeta_n+1\right) \Rightarrow \sigma_n^2 = \frac{\overline{n}}{\zeta_n+1}, \quad (4.30)$$

then from (4.27)

$$f_Z(z) = \frac{\mathrm{SIR}(\zeta_n + 1)}{\left(z + \mathrm{SIR}(\zeta_n + 1)\right)^2} \exp\left(-\zeta_n \frac{z}{z + \mathrm{SIR}(\zeta_n + 1)}\right)\left(1 + \zeta_n \frac{\mathrm{SIR}(\zeta_n + 1)}{z + \mathrm{SIR}(\zeta_n + 1)}\right) \quad (4.31)$$

where

$$\mathrm{SIR} = \frac{\overline{s}}{\overline{n}} \quad (4.32)$$

is the average signal–to–interference power ratio.

1. Without FEC

a. BPSK/QPSK

The probability of bit error for a BPSK/QPSK signal with Rayleigh fading and Ricean fading interference was evaluated numerically after substituting (4.31) into (4.13). Since the interference is assumed to be pulsed, a symbol may or may not be affected by the interference. Therefore, (3.12) applies. The probability of bit error for a Rayleigh fading signal in AWGN is obtained from (3.5) by letting $\zeta = \zeta_s = 0$.

Figure 26 shows the probability of bit error vs. SIR for BPSK/QPSK when the signal is transmitted over a Rayleigh fading channel with AWGN and Ricean fading pulsed–noise interference for various values of ζ_n and for $p = 0.5$. Figure 27 shows the probability of bit error vs. SIR for $\zeta_n = 1$ and $\zeta_n = 10$ and for various values of p. The SNR is 34 dB in both figures, and SIR ≤ 24 dB, so the assumption (4.2) stands. The particular value of SNR was selected because, in the absence of interference, it yields a probability of bit error on the order of 10^{-4}. The same criterion for the selection of the SNR was used in all subsequent plots, the ones with FEC included. In the previous chapter, for the plots with FEC, a SNR was selected that yielded a probability of bit error on the order of 10^{-7} in the absence of interference. However, given the assumption (4.2), this approach would limit significantly the range of SIR; therefore, it is not used in this chapter.

We observe that the fading of the interference signal does not affect P_b. However, P_b is affected by the variation of the interference duty cycle p, with the worst case occurring for $p = 1$.

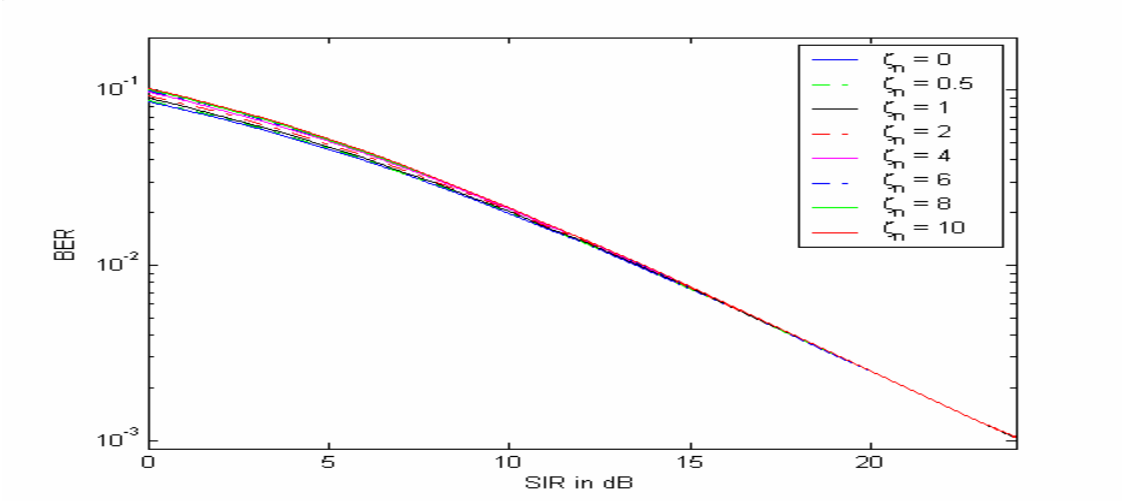

Figure 26. BPSK/QPSK transmitted over a Rayleigh fading channel with Ricean fading pulsed–noise interference $(p = 0.5)$ and AWGN.

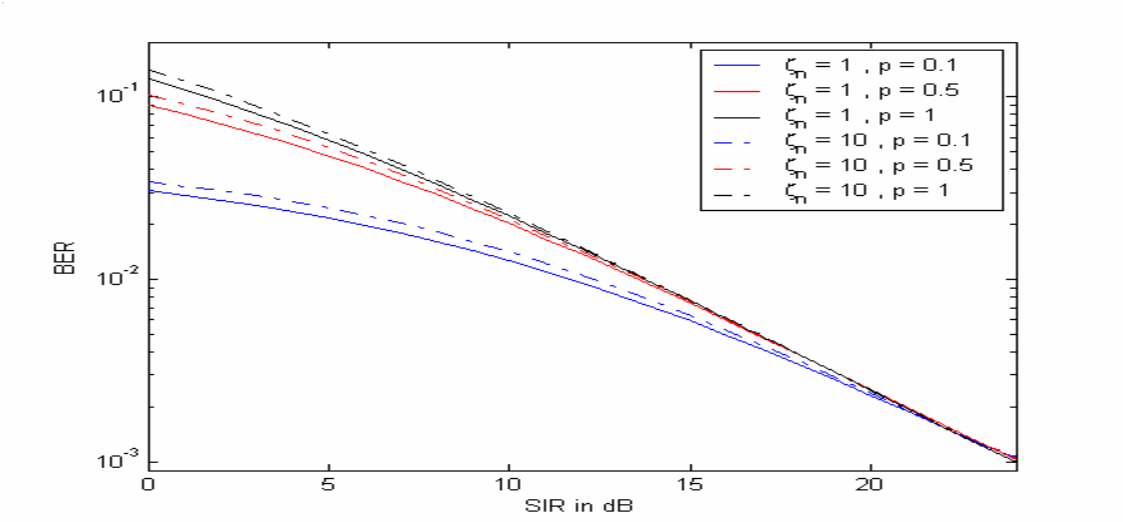

Figure 27. BPSK/QPSK transmitted over a Rayleigh fading channel with Ricean fading pulsed–noise interference and AWGN.

b. 16–QAM

Following the same reasoning as for BPSK/QPSK, we obtain the probability of bit error for a 16–QAM Rayleigh fading signal in Ricean fading interference from (3.14) by letting $E_b/N_0 = z$ and averaging over the random variable *z*. The probability of bit error for a Rayleigh fading 16–QAM signal in AWGN is obtained from (3.15) by letting $\zeta = \zeta_s = 0$.

Figure 28 shows the probability of bit error vs. SIR for 16–QAM when the signal is transmitted over a Rayleigh fading channel with AWGN and Ricean fading pulsed–noise interference for various values of ζ_n and for $p = 0.5$. Figure 29 shows the probability of bit error vs. SIR for $\zeta_n = 1$ and $\zeta_n = 10$ and for various values of p. The SNR is 35 dB for both figures and SIR ≤ 25 dB, so the assumption (4.2) stands.

Similar to BPSK/QPSK, we observe that fading of the interference does not affect P_b, but the effect of varying the parameter p is stronger for 16–QAM, and the worst case still occurs for $p = 1$.

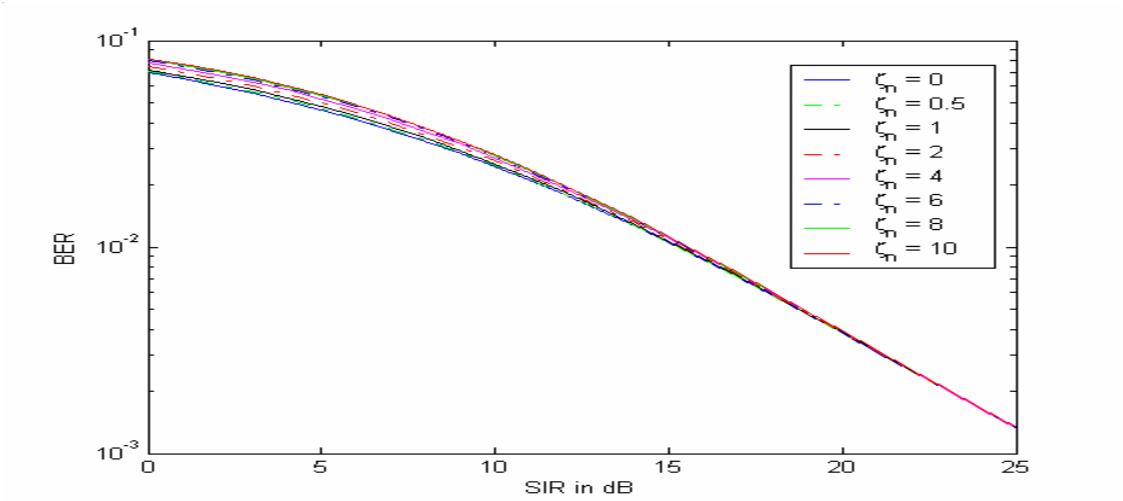

Figure 28. 16–QAM transmitted over a Rayleigh fading channel with Ricean fading pulsed–noise interference $(p = 0.5)$ and AWGN.

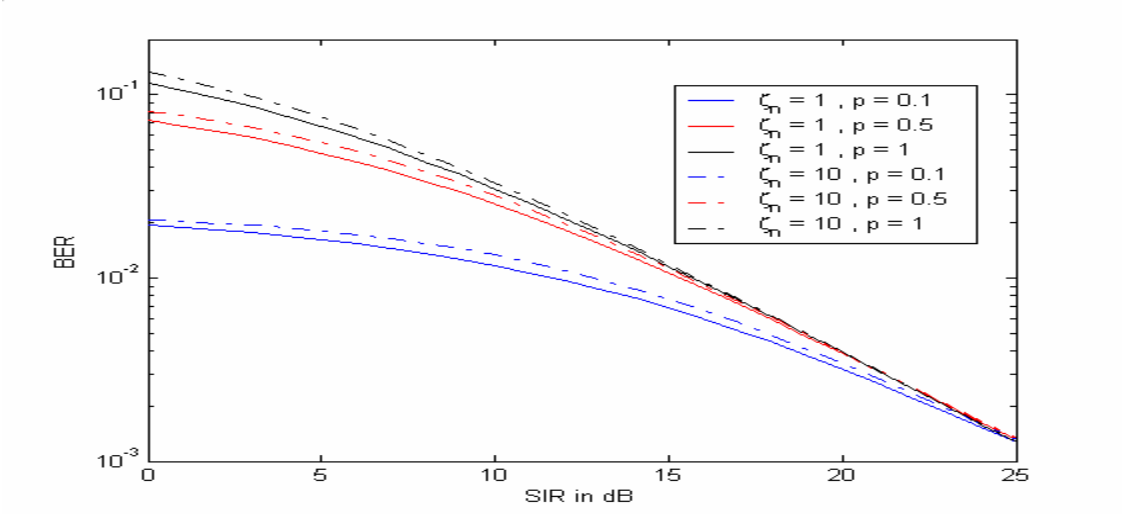

Figure 29. 16–QAM transmitted over a Rayleigh fading channel with Ricean fading pulsed–noise interference and AWGN.

c. 64–QAM

In the same manner as for 16–QAM, we obtain the probability of bit error for a 64–QAM Rayleigh fading signal in Ricean fading interference and AWGN.

Figure 30 shows the probability of bit error vs. SIR for 64–QAM when the signal is transmitted over a Rayleigh fading channel with AWGN and Ricean fading pulsed–noise interference for various values of ζ_n and for $p = 0.5$. Figure 31 shows the probability of bit error vs. SIR for $\zeta_n = 1$ and $\zeta_n = 10$ and for various values of p. The SNR is 40 dB for both figures and SIR ≤ 30 dB, so the assumption (4.2) stands.

The effect of fading and interference on performance is similar to that obtained for BPSK/QPSK and 16–QAM, i.e., no effect of the interference fading on P_b and an even stronger effect of varying the parameter p with the worst case occurring for $p = 1$.

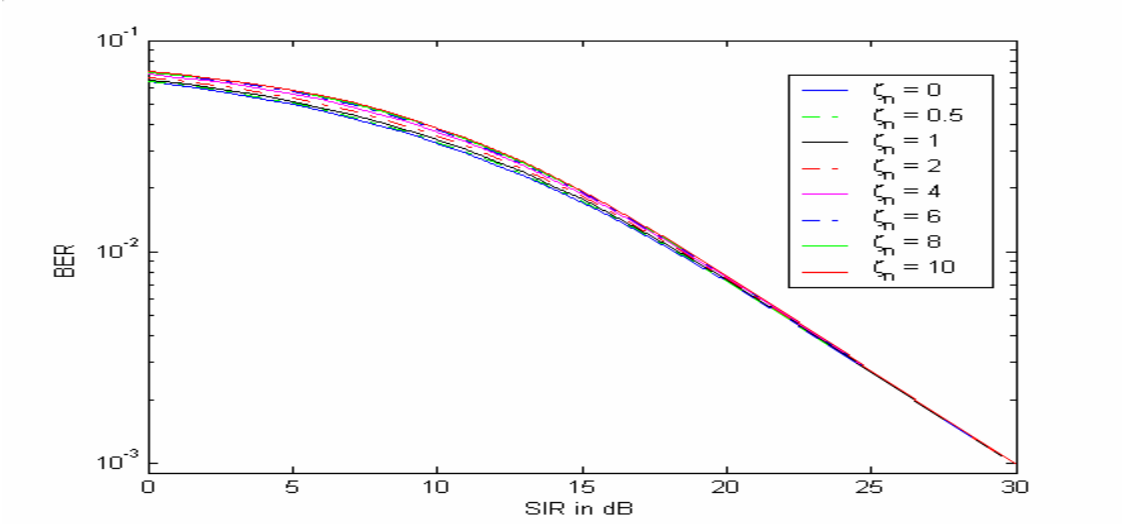

Figure 30. 64–QAM transmitted over a Rayleigh fading channel with Ricean fading pulsed–noise interference $(p = 0.5)$ and AWGN.

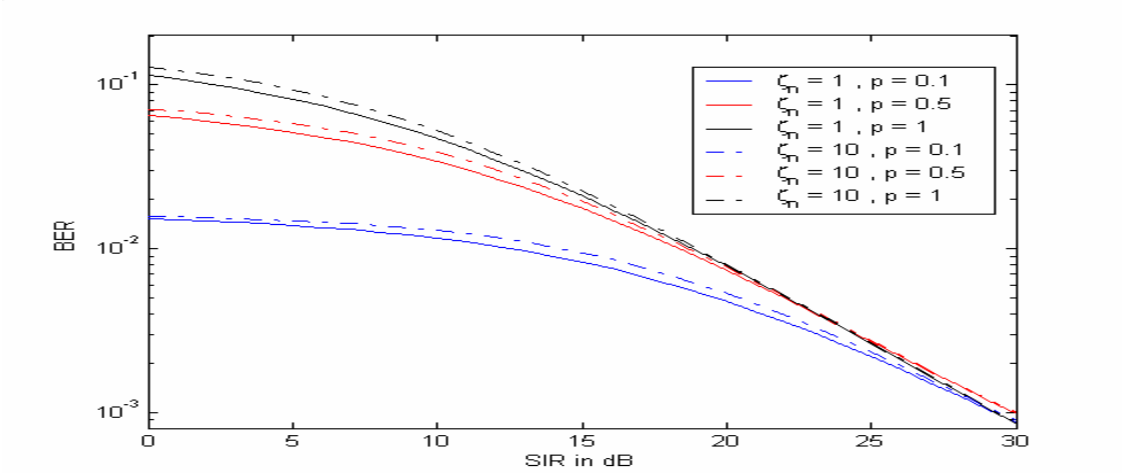

Figure 31. 64–QAM transmitted over a Rayleigh fading channel with Ricean fading pulsed–noise interference and AWGN.

2. With Convolutional Coding and Hard Decision Decoding (HDD)

a. BPSK/QPSK with Convolutional Coding and HDD r = 1/2

Figure 32 shows the probability of bit error vs. SIR for BPSK/QPSK with convolutional coding and HDD for $r = 1/2$ when the signal is transmitted over a Rayleigh fading channel with AWGN and Ricean fading pulsed–noise interference for various values of ζ_n and for $p = 0.5$. Figure 33 shows the probability of bit error vs. SIR for $\zeta_n = 1$ and $\zeta_n = 10$ and for various values of p. The SNR is 34 dB in both figures and SIR $\leq$ 24 dB, so the assumption (4.2) stands.

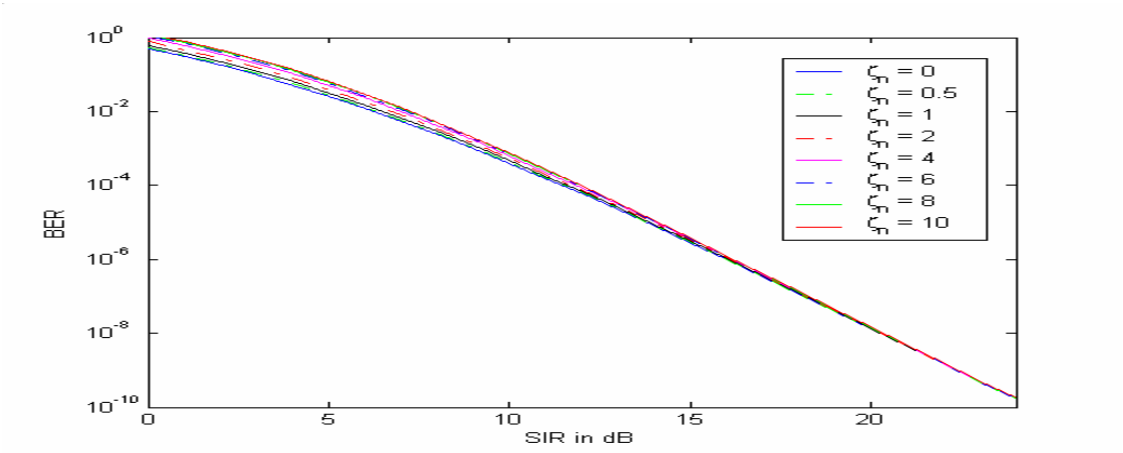

Figure 32. BPSK/QPSK with $r = 1/2$ convolutional coding and HDD transmitted over a Rayleigh fading channel with Ricean fading pulsed–noise interference $(p = 0.5)$ and AWGN.

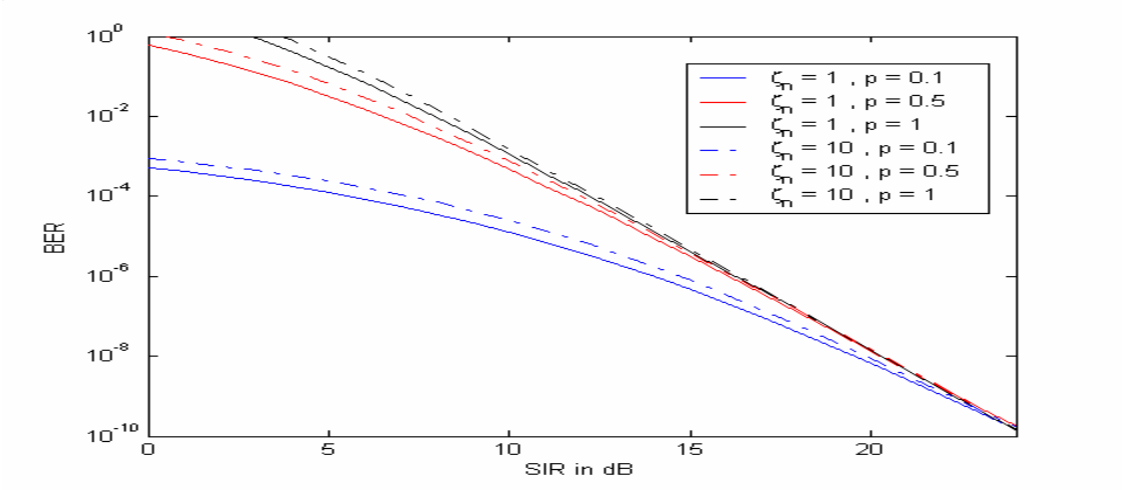

Figure 33. BPSK/QPSK with $r = 1/2$ convolutional coding and HDD transmitted over a Rayleigh fading channel with Ricean fading pulsed–noise interference and AWGN.

b. BPSK /QPSK with Convolutional Coding and HDD r = 3/4

Figure 34 shows the probability of bit error vs. SIR for BPSK/QPSK with convolutional coding and HDD for $r = 3/4$ when the signal is transmitted over a Rayleigh fading channel with AWGN and Ricean fading pulsed–noise interference for various values of ζ_n and for $p = 0.5$. Figure 35 shows the probability of bit error vs. SIR for $\zeta_n = 1$ and $\zeta_n = 10$ and for various values of p. The SNR is 34 dB in both figures and SIR $\leq$ 24 dB, so the assumption (4.2) stands.

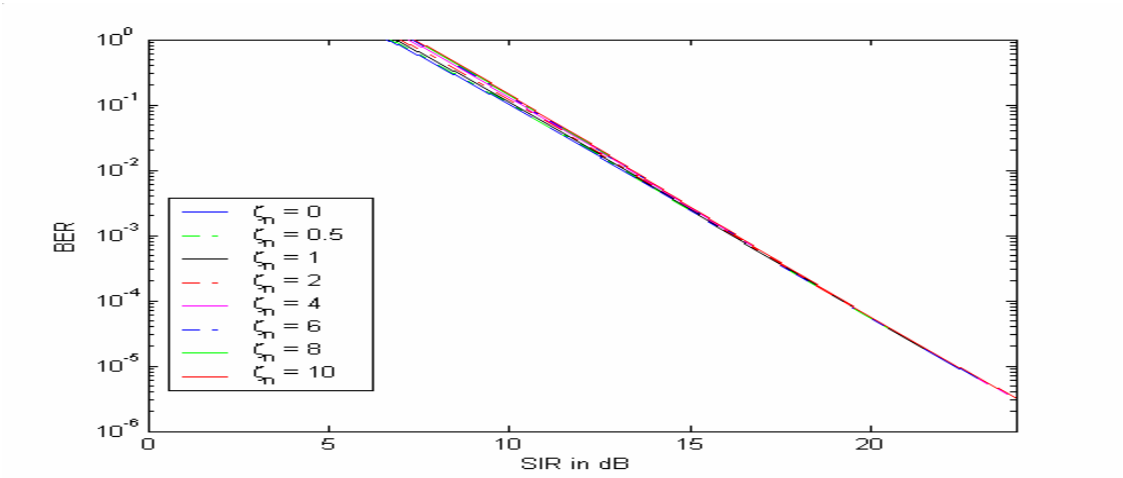

Figure 34. BPSK/QPSK with $r = 3/4$ convolutional coding and HDD transmitted over a Rayleigh fading channel with Ricean fading pulsed–noise interference $(p = 0.5)$ and AWGN.

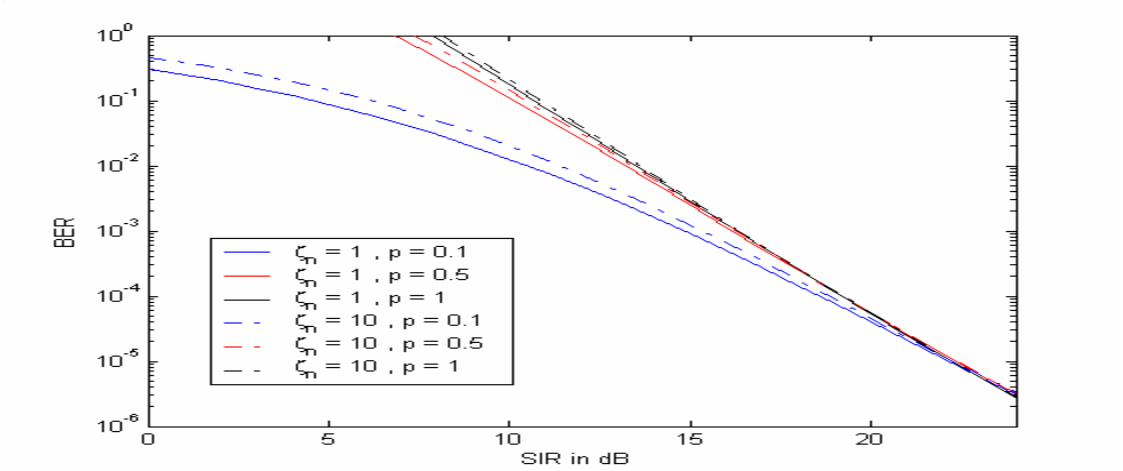

Figure 35. BPSK/QPSK with $r = 3/4$ convolutional coding and HDD transmitted over a Rayleigh fading channel with Ricean fading pulsed–noise interference and AWGN.

c. 16–QAM with Convolutional Coding and HDD r = 1/2

Figure 36 shows the probability of bit error vs. SIR for 16–QAM with convolutional coding and HDD for $r = 1/2$ when the signal is transmitted over a Rayleigh fading channel with AWGN and Ricean fading pulsed–noise interference for various values of ζ_n and for $p = 0.5$. Figure 37 shows the probability of bit error vs. SIR for $\zeta_n = 1$ and $\zeta_n = 10$ and for various values of p. The SNR is 35 dB for both figures and SIR $\leq$ 25 dB.

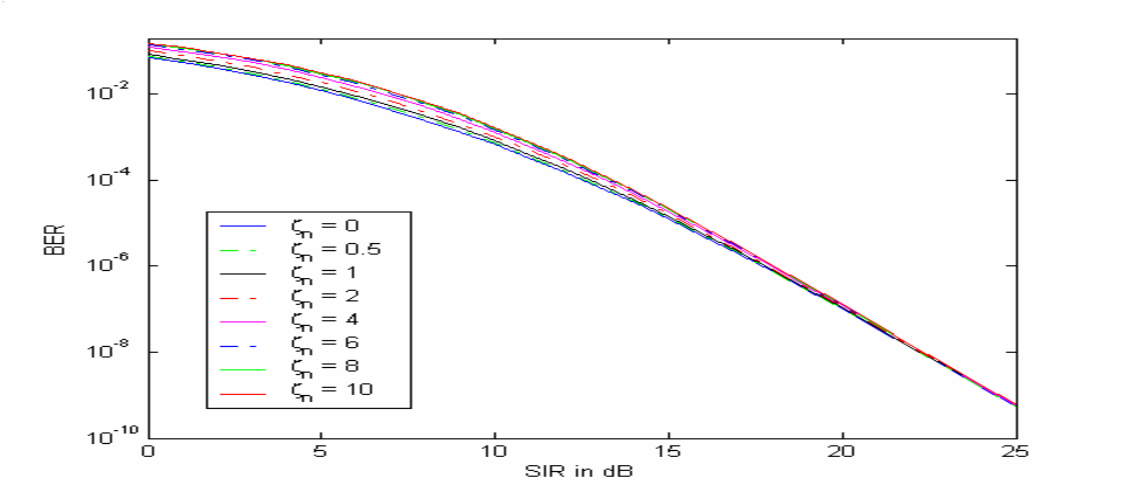

Figure 36. 16–QAM with $r = 1/2$ convolutional coding and HDD transmitted over a Rayleigh fading channel with Ricean fading pulsed–noise interference ($p = 0.5$) and AWGN.

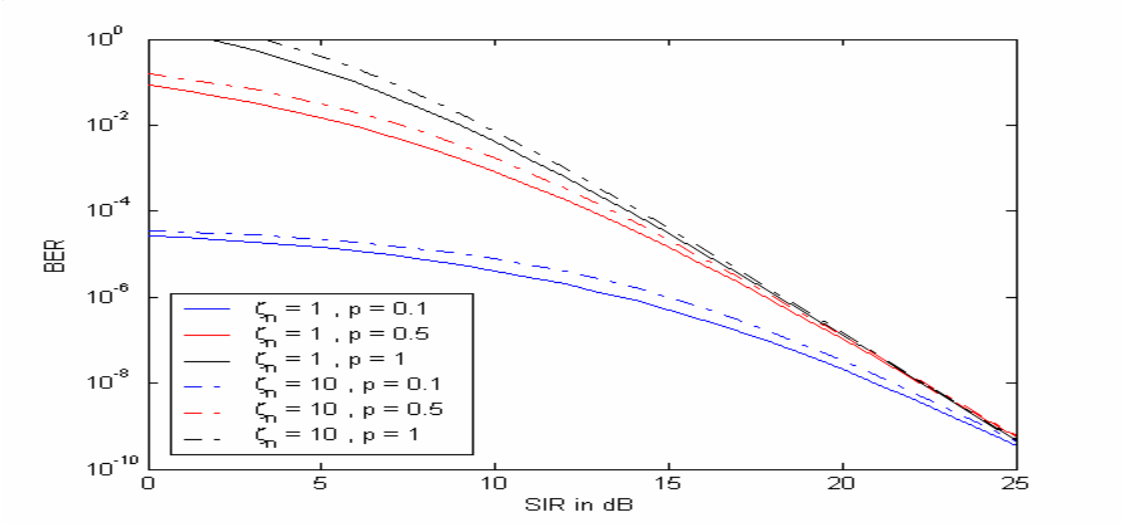

Figure 37. 16–QAM with $r = 1/2$ convolutional coding and HDD transmitted over a Rayleigh fading channel with Ricean fading pulsed–noise interference and AWGN.

d. 16–QAM with Convolutional Coding and HDD r = 3/4

Figure 38 shows the probability of bit error vs. SIR for 16–QAM with convolutional coding and HDD for $r = 3/4$ when the signal is transmitted over a Rayleigh fading channel with AWGN and Ricean fading pulsed–noise interference for various values of ζ_n and for $p = 0.5$. Figure 39 shows the probability of bit error vs. SIR for $\zeta_n = 1$ and ζ_n=10 and for various values of p. The SNR is 35 dB for both figures and SIR $\leq$ 25 dB.

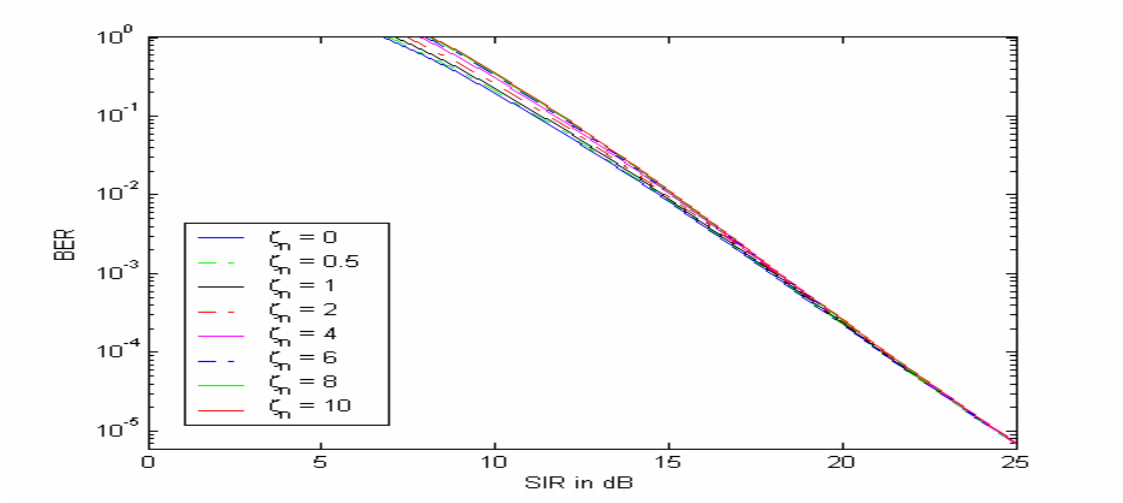

Figure 38. 16–QAM with $r = 3/4$ convolutional coding and HDD transmitted over a Rayleigh fading channel with Ricean fading pulsed–noise interference $(p = 0.5)$ and AWGN.

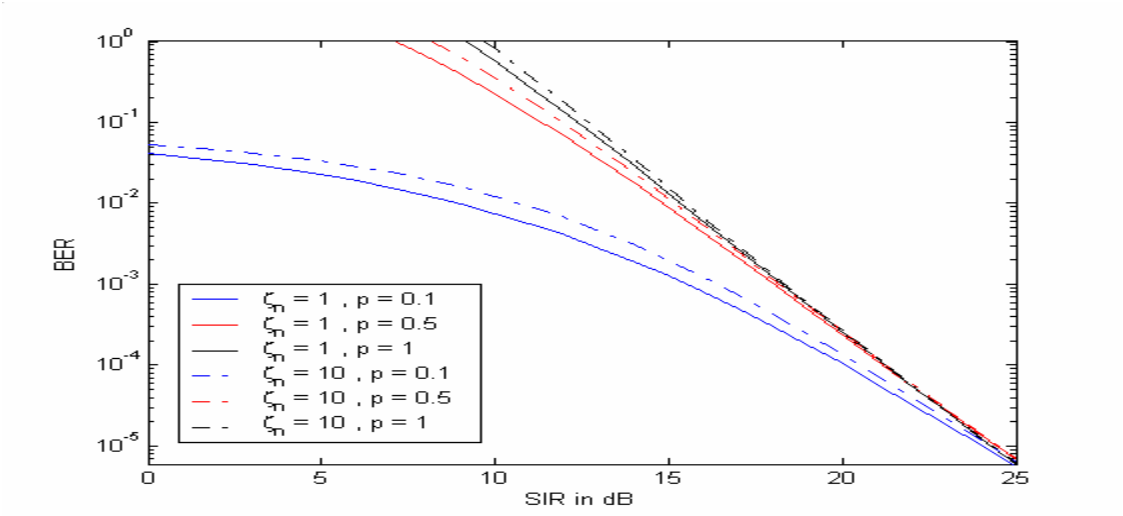

Figure 39. 16–QAM with $r = 3/4$ convolutional coding and HDD transmitted over a Rayleigh fading channel with Ricean fading pulsed–noise interference and AWGN.

e. 64–QAM with Convolutional Coding and HDD $r = 2/3$

Figure 40 shows the probability of bit error vs. SIR for 64–QAM with convolutional coding and HDD for $r = 2/3$ when the signal is transmitted over a Rayleigh fading channel with AWGN and Ricean fading pulsed–noise interference for various values of ζ_n and for $p = 0.5$. Figure 41 shows the probability of bit error vs. SIR

for $\zeta_n = 1$ and $\zeta_n = 10$ and for various values of p. The SNR is 40 dB for both figures and SIR ≤ 30 dB, so the assumption (4.2) stands.

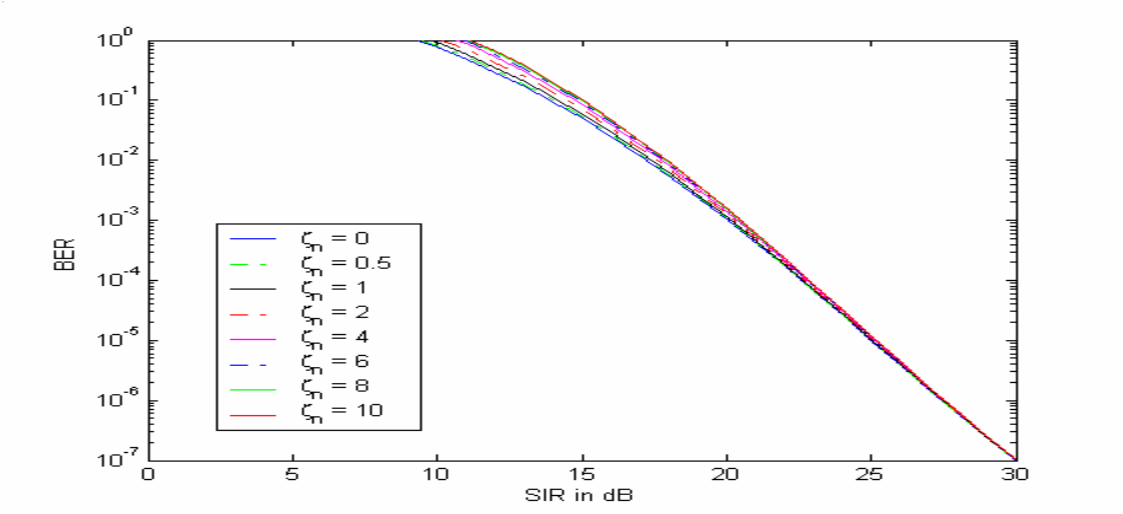

Figure 40. 64–QAM with $r = 2/3$ convolutional coding and HDD transmitted over a Rayleigh fading channel with Ricean fading pulsed–noise interference $(p = 0.5)$ and AWGN.

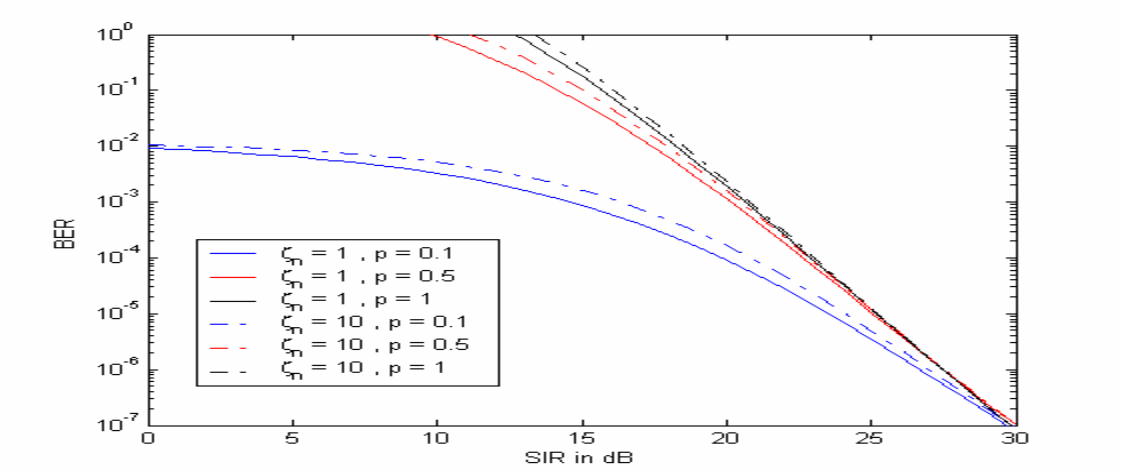

Figure 41. 64–QAM with $r = 2/3$ convolutional coding and HDD transmitted over a Rayleigh fading channel with Ricean fading pulsed–noise interference and AWGN.

f. 64–QAM with Convolutional Coding and HDD r = 3/4

Figure 42 shows the probability of bit error vs. SIR for 64–QAM with convolutional coding and HDD for $r = 3/4$ when the signal is transmitted over a Rayleigh fading channel with AWGN and Ricean fading pulsed–noise interference for

various values of ζ_n and for $p = 0.5$. Figure 43 shows the probability of bit error vs. SIR for $\zeta_n = 1$ and $\zeta_n = 10$ and for various values of p. The SNR is 40 dB for both figures and SIR ≤ 30 dB.

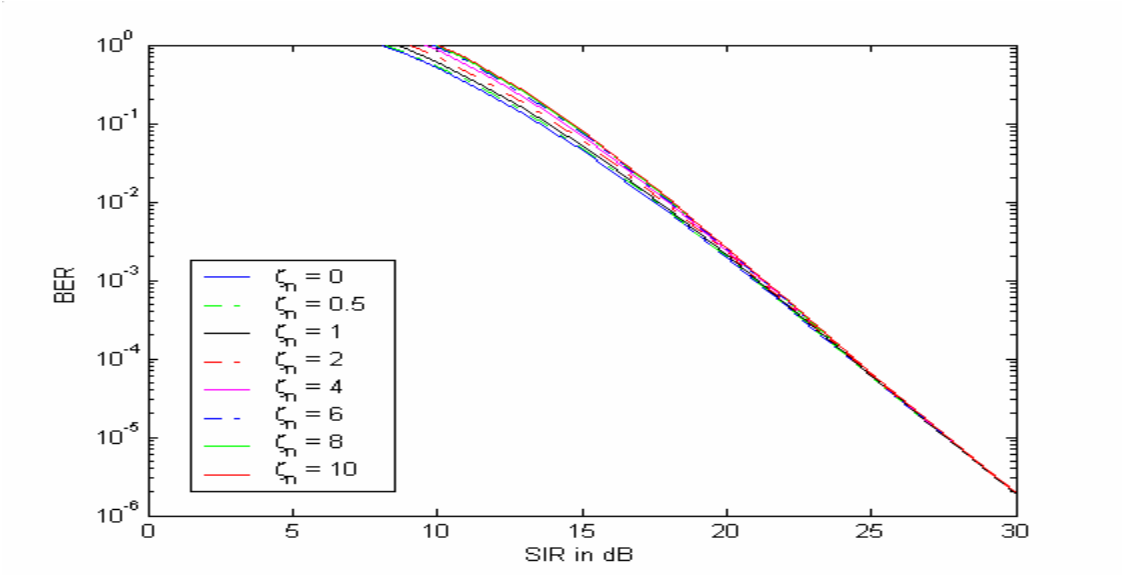

Figure 42. 64–QAM with $r = 3/4$ convolutional coding and HDD transmitted over a Rayleigh fading channel with Ricean fading pulsed–noise interference $(p = 0.5)$ and AWGN.

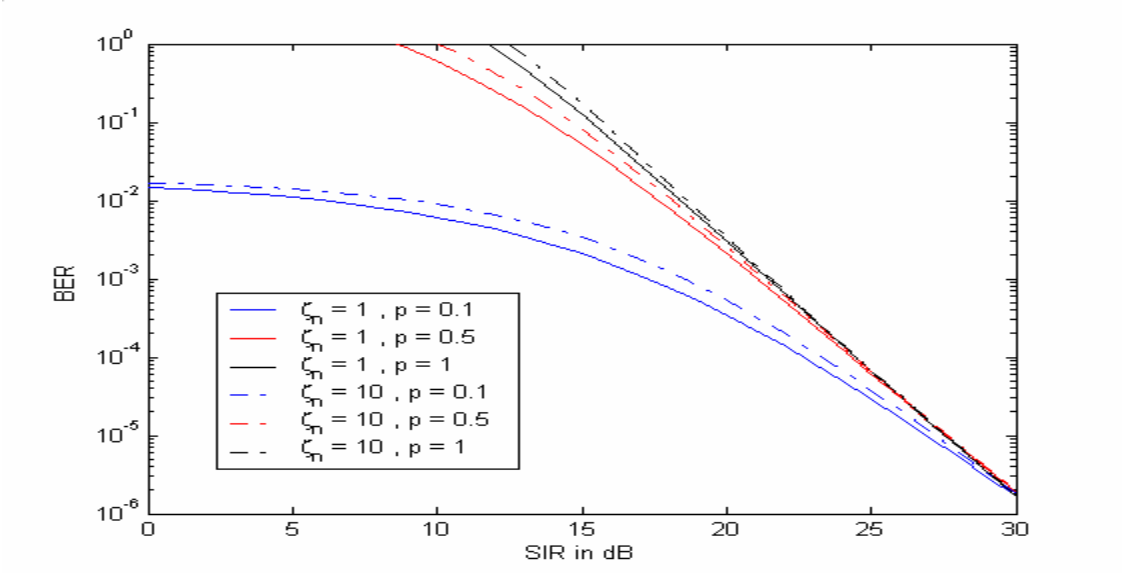

Figure 43. 64–QAM with $r = 3/4$ convolutional coding and HDD transmitted over a Rayleigh fading channel with Ricean fading pulsed–noise interference and AWGN.

Except for the improvement in performance with respect to P_b, the use of convolutional coding with HDD does not alter the picture observed for the non–FEC cases. Performance is only slightly affected by the interference fading, but is affected by the pulsed interference duty cycle p. The worst case for all modulation schemes with convolutional coding and HDD occurs for $p = 1$.

D. PERFORMANCE ANALYSIS FOR A RICEAN FADING SIGNAL WITH RAYLEIGH FADING PULSED–NOISE INTERFERENCE

By allowing $\alpha_n = 0$ in the general case, the useful signal experiences Ricean fading and the interference signal is subject to Rayleigh fading. From (4.18)

$$f_Z(z) = \frac{1}{4\sigma_s^2\sigma_n^2}\exp\left(\frac{-\alpha_s^2}{2\sigma_s^2}\right)\int_0^\infty n\exp\left(\frac{-zn}{2\sigma_s^2}+\frac{-n}{2\sigma_n^2}\right)J_0\left(\frac{j\alpha_s\sqrt{zn}}{\sigma_s^2}\right)J_0(0)\,dn\,. \tag{4.33}$$

Using once more the identity (3.31) with

$$m = 1, \tag{4.34}$$

$$n = 0, \tag{4.35}$$

$$\nu = \frac{z}{2\sigma_s^2}+\frac{1}{2\sigma_n^2} = \frac{z\sigma_n^2+\sigma_s^2}{2\sigma_s^2\sigma_n^2}, \tag{4.36}$$

and

$$2\beta = j\frac{\alpha_n\sqrt{z}}{\sigma_s^2} \Rightarrow \beta^2 = -\frac{\alpha_s^2 z}{\sigma_s^2} \Rightarrow \frac{\beta^2}{\nu} = -\frac{\alpha_s^2\sigma_n^2 z}{2\sigma_s^2\left(z\sigma_n^2+\sigma_s^2\right)}, \tag{4.37}$$

and the identity (4.26), we get

$$f_Z(z) = \frac{\sigma_n^2\sigma_s^2}{\left(z\sigma_n^2+\sigma_s^2\right)^2}\exp\left(-\frac{\alpha_s^2}{2\sigma_s^2}\frac{\sigma_s^2}{z\sigma_n^2+\sigma_s^2}\right)\left(1+\frac{\alpha_s^2}{2\sigma_s^2}\frac{z\sigma_n^2}{z\sigma_n^2+\sigma_s^2}\right). \tag{4.38}$$

Since

$$\zeta_s = \frac{\alpha_s^2}{2\sigma_s^2}, \tag{4.39}$$

$$\overline{s} = \overline{a_c^2} = \alpha_s^2 + 2\sigma_s^2 = 2\sigma_s^2\left(\zeta_s+1\right) \Rightarrow \sigma_s^2 = \frac{\overline{s}}{2\left(\zeta_s+1\right)}, \tag{4.40}$$

and

$$\overline{n} = \overline{\sigma_I^2} = 2\sigma_n^2 \Rightarrow \sigma_n^2 = \frac{\overline{n}}{2}, \tag{4.41}$$

using (4.32), we get

$$f_Z(z) = \frac{\mathrm{SIR}(\zeta_s + 1)}{\left(z(\zeta_s + 1) + \mathrm{SIR}\right)^2} \exp\left(-\zeta_s \frac{\mathrm{SIR}}{z(\zeta_s + 1) + \mathrm{SIR}}\right)\left(1 + \zeta_s \frac{z(\zeta_s + 1)}{z(\zeta_s + 1) + \mathrm{SIR}}\right). \quad (4.42)$$

Equation (4.42) is now substituted into (4.13), which is then evaluated numerically.

1. Without Forward Error Correction Coding (FEC)

a. BPSK/QPSK

The probability of bit error vs. SIR for BPSK/QPSK when the signal is transmitted over a Ricean fading channel with AWGN and Rayleigh fading pulsed noise–like interference is plotted in Figure 44 for various values of the channel parameter ζ_s and for $p = 0.5$. In Figure 45, the probability of bit error vs. SIR is plotted for various values of p and $\zeta_s = 1$, $\zeta_s = 10$. The SNR is 32 dB for both figures and $\mathrm{SIR} \le 22$ dB so the assumption (4.2) stands.

Performance in terms of P_b improves while ζ_s increases. For a low value of ζ_s, $p = 1$ is the worst case and the parameter p does not affect performance for $\mathrm{SIR} > 15$ dB. For larger ζ_s values and $\mathrm{SIR} > 5$ dB, low values of p $(p = 0.1)$ represent the worst case.

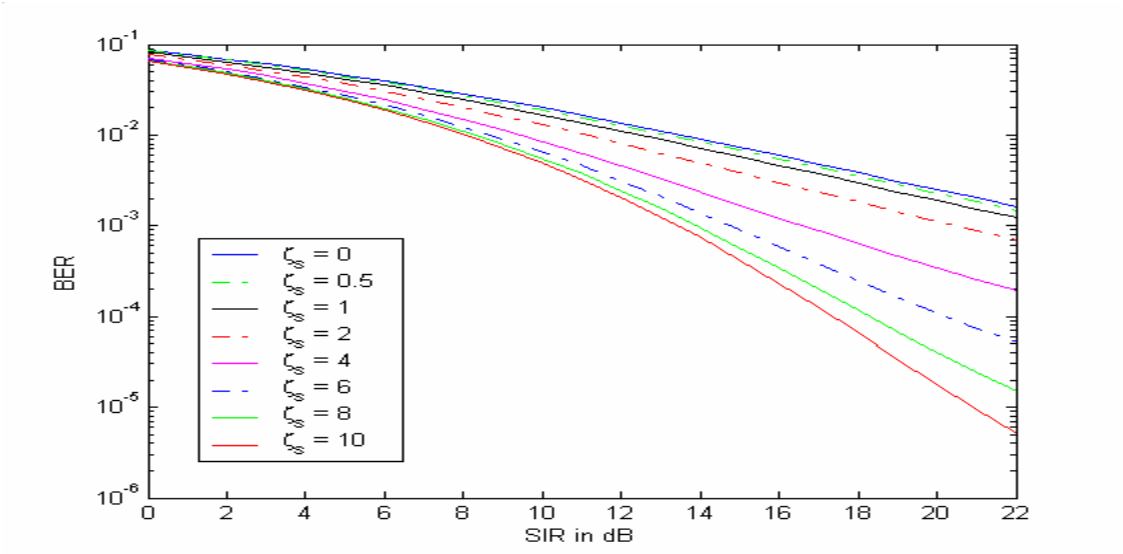

Figure 44. BPSK/QPSK transmitted over a Ricean fading channel with Rayleigh fading pulsed–noise interference $(p = 0.5)$ and AWGN.

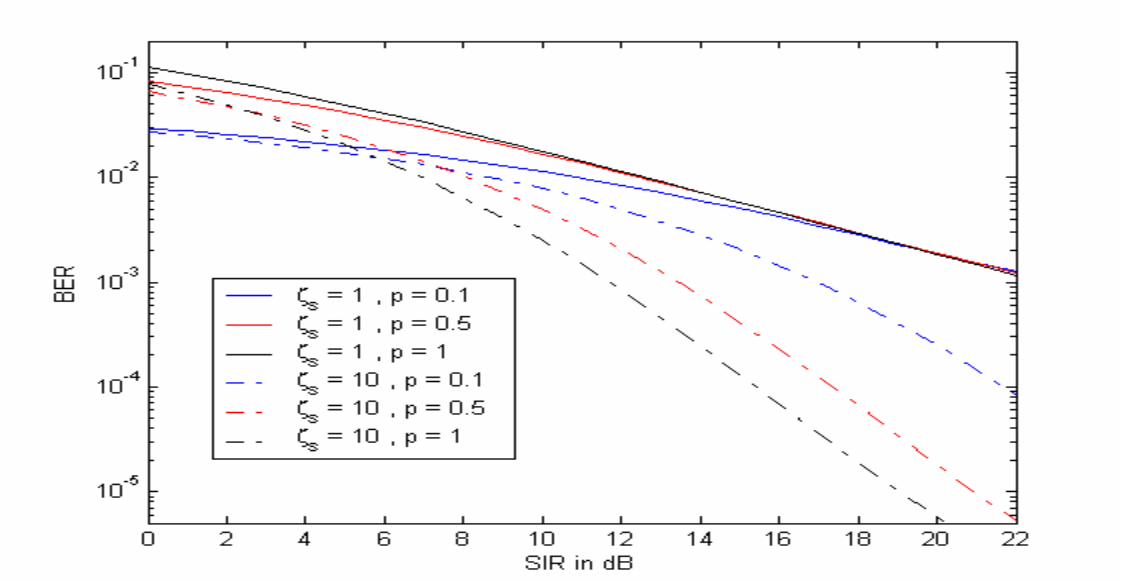

Figure 45. BPSK/QPSK transmitted over a Ricean fading channel with Rayleigh fading pulsed–noise interference and AWGN.

b. 16–QAM

The probability of bit error vs. SIR for 16–QAM when the signal is transmitted over a Ricean fading channel with AWGN and Rayleigh fading pulsed noise–like interference is plotted in Figure 46 for various values of the channel parameter ζ_s and for $p = 0.5$. In Figure 47, the probability of bit error vs. SIR is plotted for various values of p and for $\zeta_s = 1$, $\zeta_s = 10$. The SNR is 35 dB for both figures and SIR $\leq$ 25 dB.

As for BPSK/QPSK, performance in terms of P_b improves while ζ_s increases. For a low value of ζ_s, $p = 1$ is the worst case and the parameter p does not affect performance for SIR > 20 dB. For larger ζ_s values and SIR > 10 dB, low values of p $(p = 0.1)$ represent the worst case.

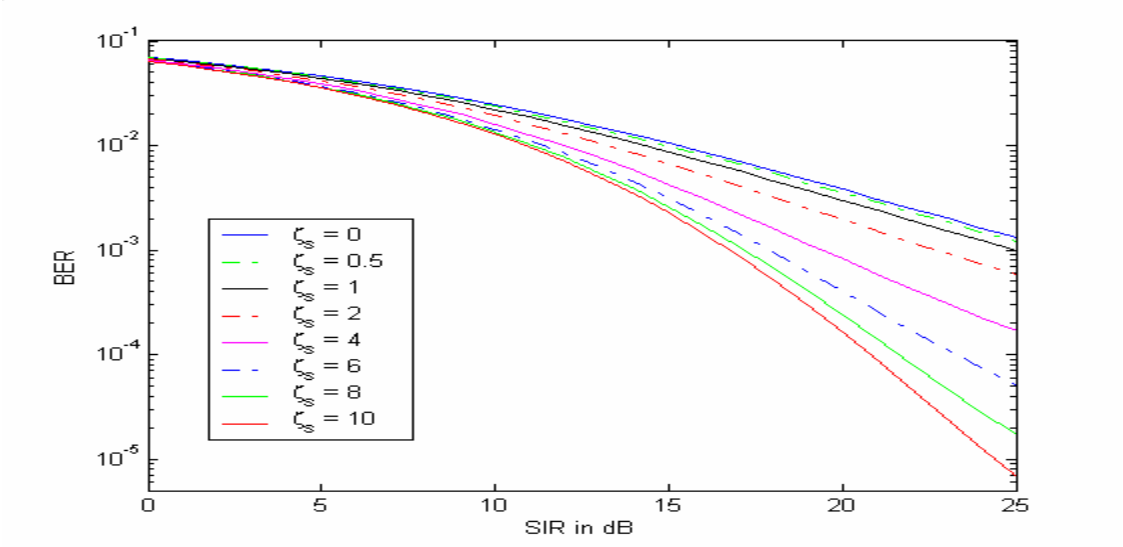

Figure 46. 16–QAM transmitted over a Ricean fading channel with Rayleigh fading pulsed–noise interference $(p = 0.5)$ and AWGN.

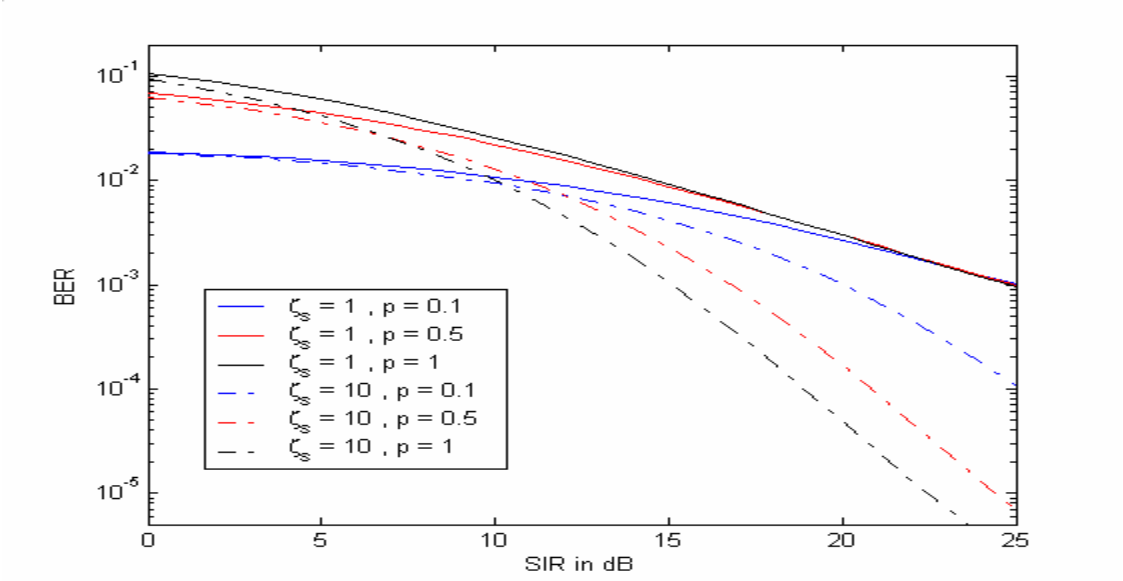

Figure 47. 16–QAM transmitted over a Ricean fading channel with Rayleigh fading pulsed–noise interference and AWGN.

c. 64–QAM

The probability of bit error vs. SIR for 64–QAM when the signal is transmitted over a Ricean fading channel with AWGN and Rayleigh fading pulsed noise–like interference is plotted in Figure 48 for various values of the channel parameter ζ_s and for

$p = 0.5$. In Figure 49, the probability of bit error vs. SIR is plotted for various values of p and for $\zeta_s = 1,\ \zeta_s = 10$. The SNR is 38 dB for both figures and SIR ≤ 28 dB.

Similar to BPSK/QPSK and 16–QAM, performance in terms of P_b improves while ζ_s increases. For a low value of ζ_s, $p = 1$ is the worst case and the parameter p does not affect performance for SIR > 25 dB. For larger ζ_s values and SIR > 15 dB, low values of p $(p = 0.1)$ represent the worst case.

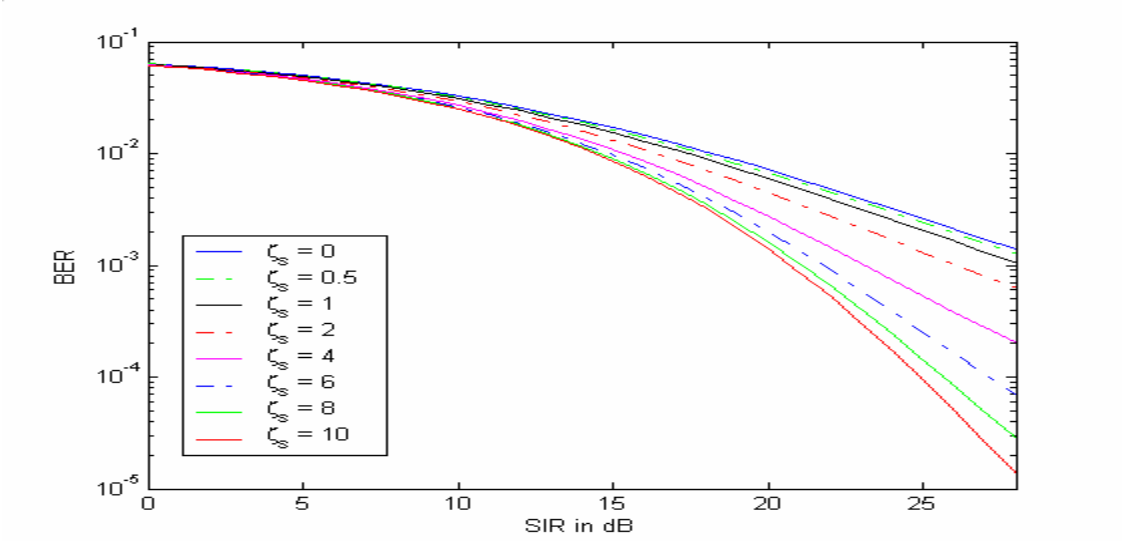

Figure 48. 64–QAM transmitted over a Ricean fading channel with Rayleigh fading pulsed–noise interference $(p = 0.5)$ and AWGN.

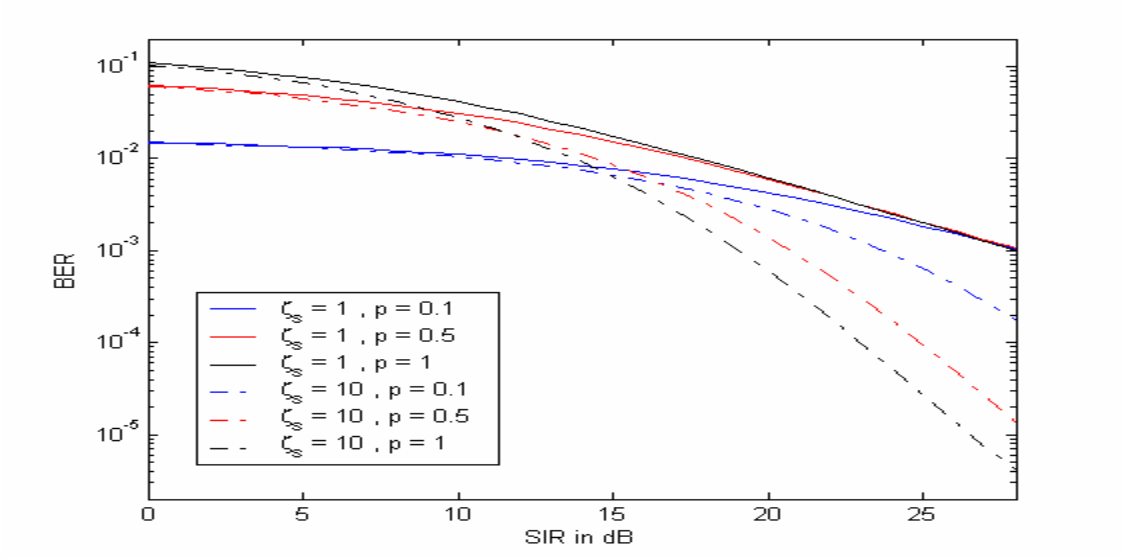

Figure 49. 64–QAM transmitted over a Ricean fading channel with Rayleigh fading pulsed–noise interference and AWGN.

2. With Convolutional Coding and Hard Decision Decoding (HDD)

a. BPSK/QPSK with Convolutional Coding and HDD for $r = 1/2$

The probability of bit error vs. SIR for BPSK/QPSK with convolutional coding and HDD for $r = 1/2$ when the signal is transmitted over a Ricean fading channel with AWGN and Rayleigh fading pulsed noise–like interference is plotted in Figure 50 for various values of the channel parameter ζ_s and for $p = 0.5$. In Figure 51, the probability of bit error vs. SIR is plotted for various values of p and $\zeta_s = 1$, $\zeta_s = 10$. The SNR is 32 dB for both figures and SIR ≤ 22 dB.

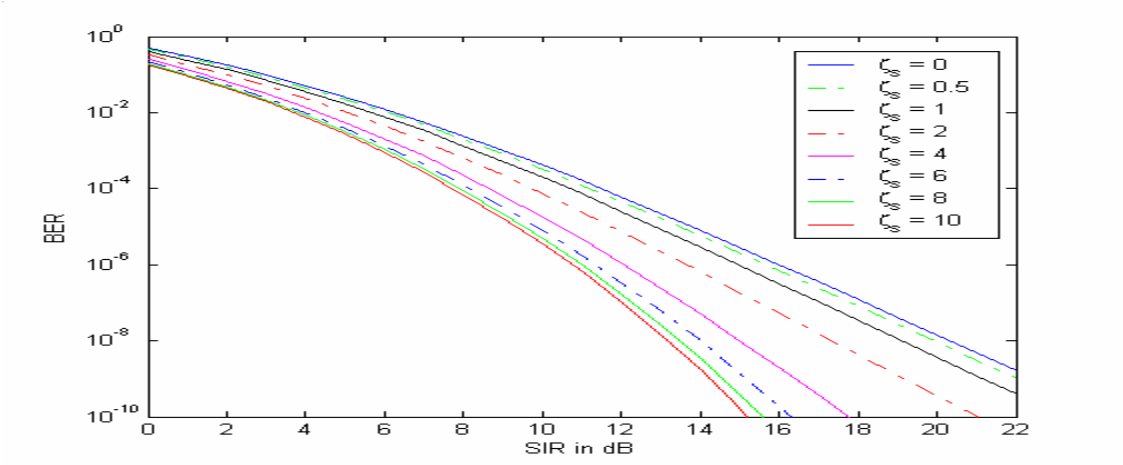

Figure 50. BPSK/QPSK with $r = 1/2$ convolutional coding and HDD transmitted over a Ricean fading channel with Rayleigh fading pulsed–noise interference $(p = 0.5)$ and AWGN.

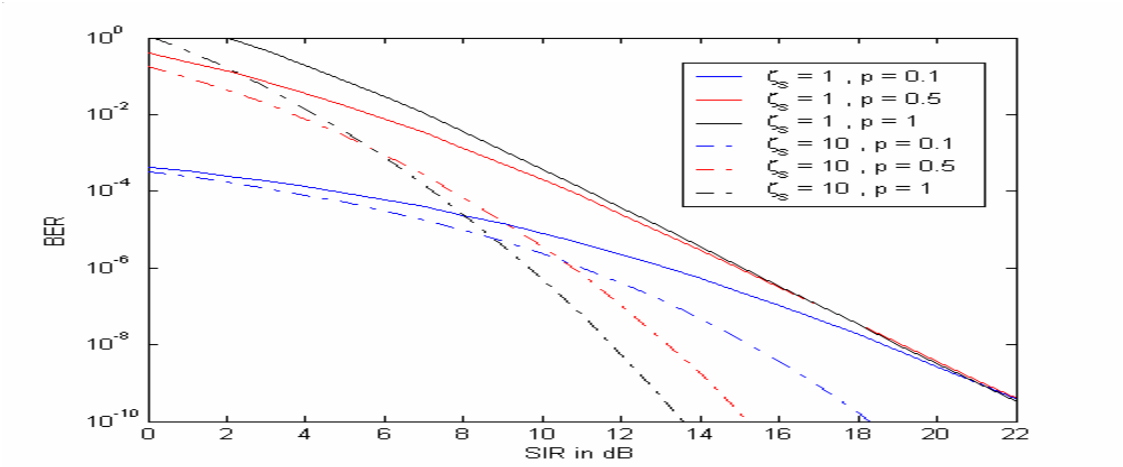

Figure 51. BPSK/QPSK with $r = 1/2$ convolutional coding and HDD transmitted over a Ricean fading channel with Rayleigh fading pulsed–noise interference and AWGN.

b. BPSK/QPSK with Convolutional Coding and HDD for $r = 3/4$

The probability of bit error vs. SIR for BPSK/QPSK with convolutional coding and HDD for $r = 3/4$ when the signal is transmitted over a Ricean fading channel with AWGN and Rayleigh fading pulsed noise–like interference is plotted in Figure 52 for various values of the channel parameter ζ_s and for $p = 0.5$. In Figure 53, the probability of bit error vs. SIR is plotted for various values of p and $\zeta_s = 1$, $\zeta_s = 10$. The SNR is 32 dB for both figures and SIR $\leq$ 22 dB.

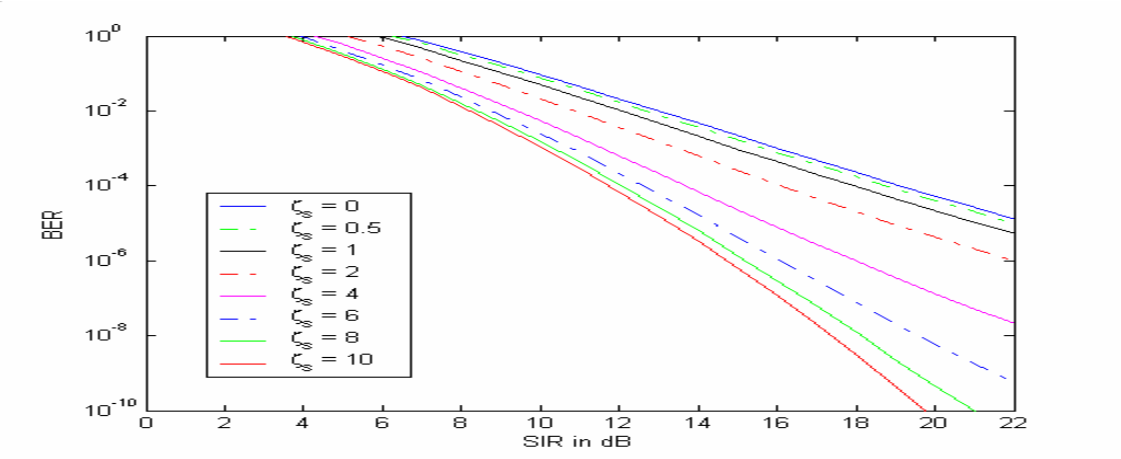

Figure 52. BPSK/QPSK with $r = 3/4$ convolutional coding and HDD transmitted over a Ricean fading channel with Rayleigh fading pulsed–noise interference $(p = 0.5)$ and AWGN.

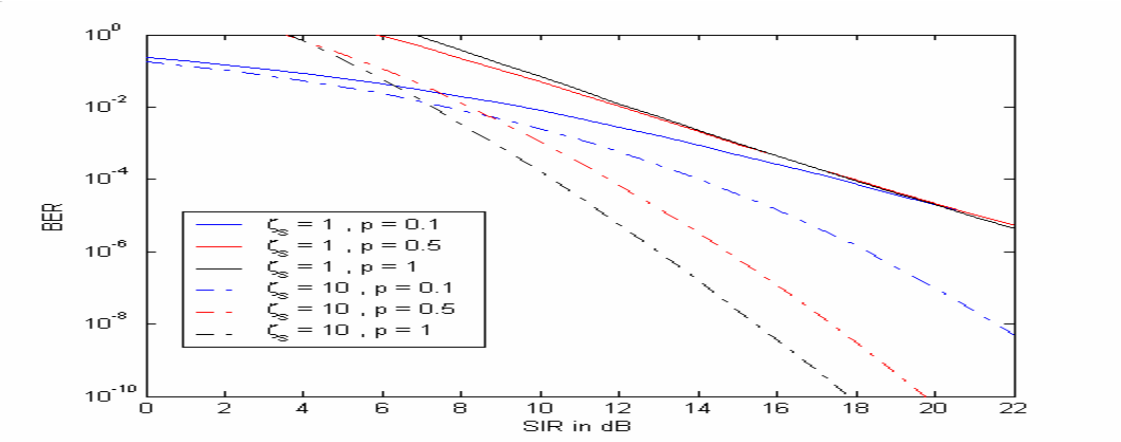

Figure 53. BPSK/QPSK with $r = 3/4$ convolutional coding and HDD transmitted over a Ricean fading channel with Rayleigh fading pulsed–noise interference and AWGN.

c. 16–QAM with Convolutional Coding and HDD for $r = 1/2$

The probability of bit error vs. SIR for 16–QAM with convolutional coding and HDD for $r = 1/2$ when the signal is transmitted over a Ricean fading channel with AWGN and Rayleigh fading pulsed noise–like interference is plotted in Figure 54 for various values of the channel parameter ζ_s and for $p = 0.5$. In Figure 55, the probability of bit error vs. SIR is plotted for various values of p and for $\zeta_s = 1,\ \zeta_s = 10$. The SNR is 35 dB for both figures and SIR $\leq$ 25 dB.

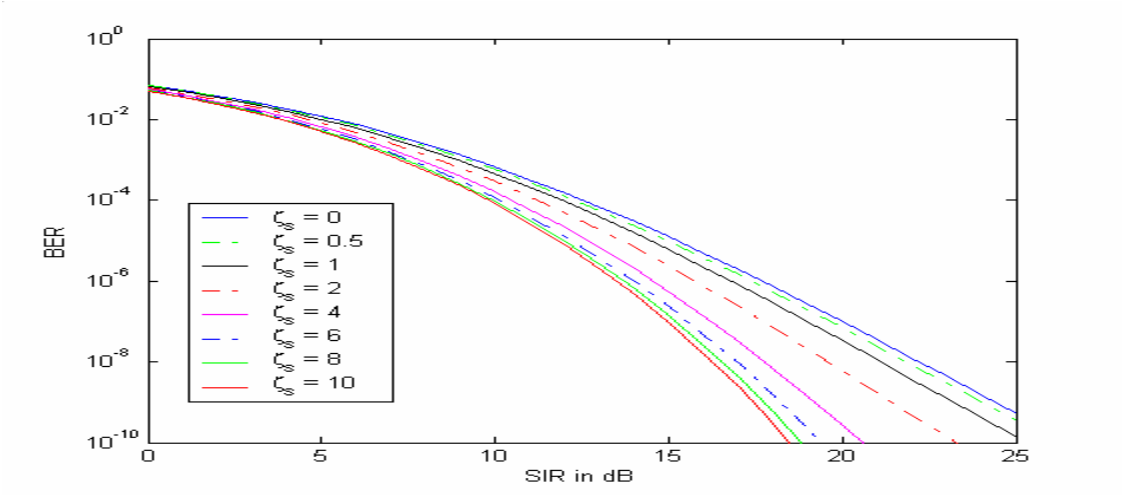

Figure 54. 16–QAM with $r = 1/2$ convolutional coding and HDD transmitted over a Ricean fading channel with Rayleigh fading pulsed–noise interference $(p = 0.5)$ and AWGN.

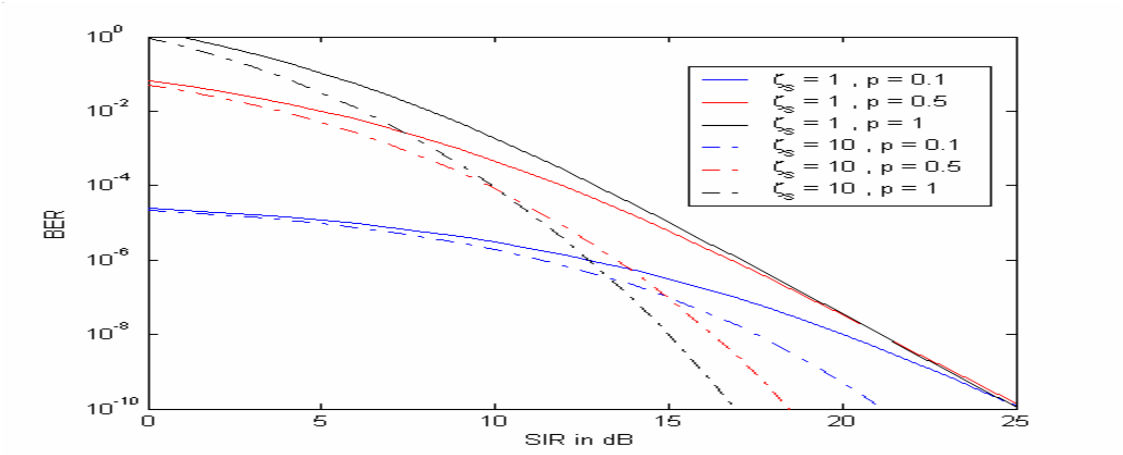

Figure 55. 16–QAM with $r = 1/2$ convolutional coding and HDD transmitted over a Ricean fading channel with Rayleigh fading pulsed–noise interference and AWGN.

d. 16–QAM with Convolutional Coding and HDD for $r = 3/4$

The probability of bit error vs. SIR for 16–QAM with convolutional coding and HDD for $r = 3/4$ when the signal is transmitted over a Ricean fading channel with AWGN and Rayleigh fading pulsed noise–like interference is plotted in Figure 56 for various values of the channel parameter ζ_s and for $p = 0.5$. In Figure 57, the probability of bit error vs. SIR is plotted for various values of p and for $\zeta_s = 1$, $\zeta_s = 10$. The SNR is 35 dB for both figures and SIR $\leq$ 25 dB.

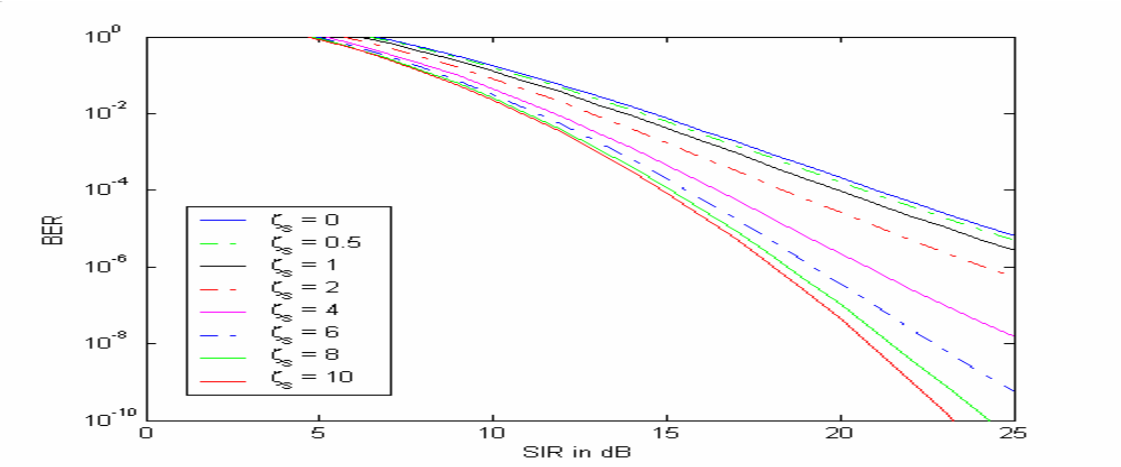

Figure 56. 16–QAM with $r = 3/4$ convolutional coding and HDD transmitted over a Ricean fading channel with Rayleigh fading pulsed–noise interference $(p = 0.5)$ and AWGN.

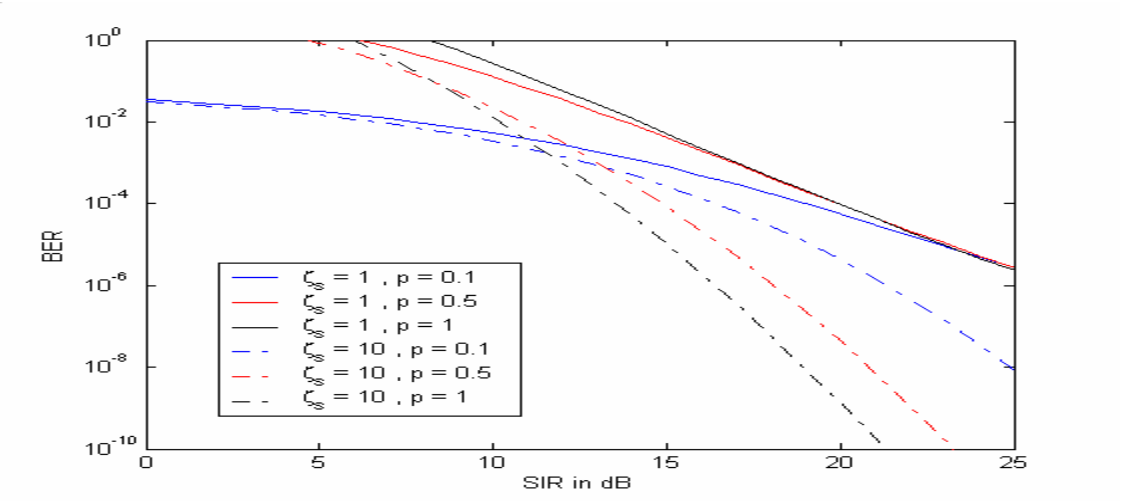

Figure 57. 16–QAM with $r = 3/4$ convolutional coding and HDD transmitted over a Ricean fading channel with Rayleigh fading pulsed–noise interference and AWGN.

e. 64–QAM with Convolutional Coding and HDD for $r = 2/3$

The probability of bit error vs. SIR for 64–QAM with convolutional coding and HDD for $r = 2/3$ when the signal is transmitted over a Ricean fading channel with AWGN and Rayleigh fading pulsed noise–like interference is plotted in Figure 58 for various values of the channel parameter ζ_s and for $p = 0.5$. In Figure 59, the probability of bit error vs. SIR is plotted for various values of p and for $\zeta_s = 1$, $\zeta_s = 10$. The SNR is 38 dB for both figures and SIR ≤ 28 dB.

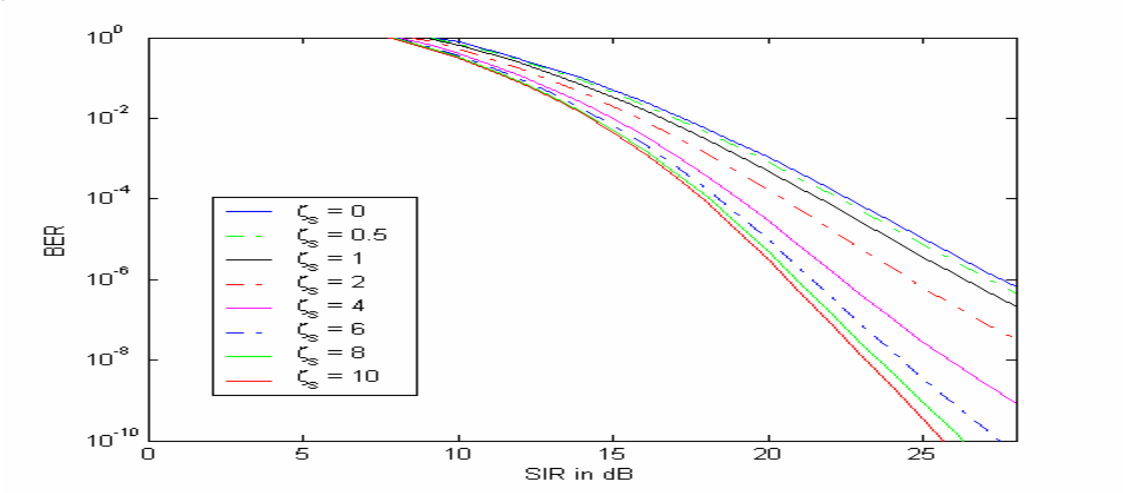

Figure 58. 64–QAM with $r = 2/3$ convolutional coding and HDD transmitted over a Ricean fading channel with Rayleigh fading pulsed–noise interference $(p = 0.5)$ and AWGN.

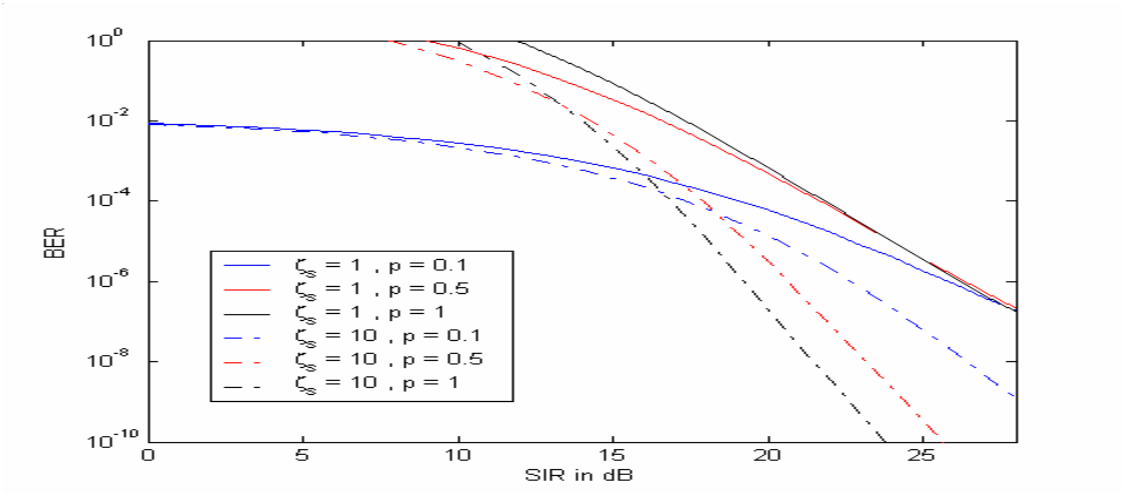

Figure 59. 64–QAM with $r = 2/3$ convolutional coding and HDD transmitted over a Ricean fading channel with Rayleigh fading pulsed–noise interference and AWGN.

f. 64–QAM with Convolutional Coding and HDD for $r = 3/4$

The probability of bit error vs. SIR for 64–QAM with convolutional coding and HDD for $r = 3/4$ when the signal is transmitted over a Ricean fading channel with AWGN and Rayleigh fading pulsed noise–like interference is plotted in Figure 60 for various values of the channel parameter ζ_s and for $p = 0.5$. In Figure 61, the probability of bit error vs. SIR is plotted for various values of p and for $\zeta_s = 1$, $\zeta_s = 10$. The SNR is 38 dB for both figures and SIR ≤ 28 dB.

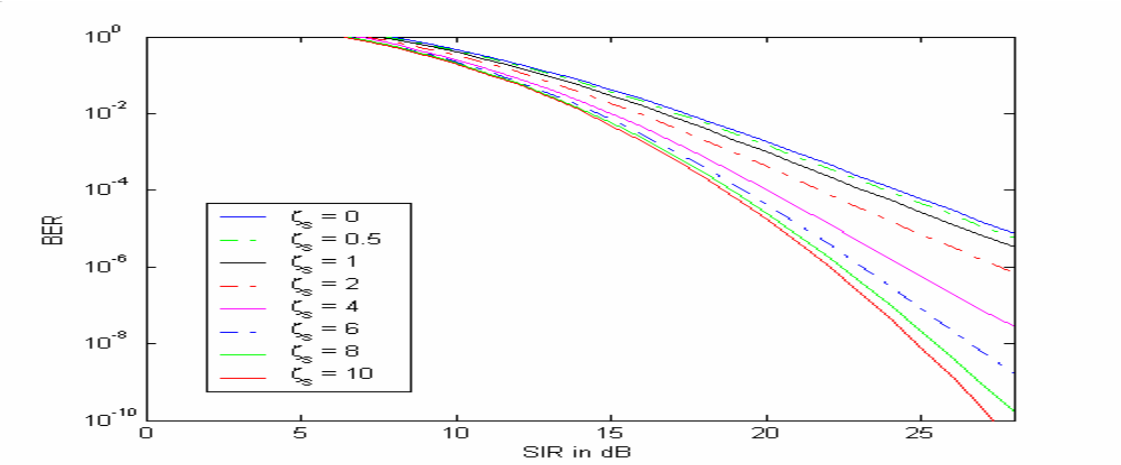

Figure 60. 64–QAM with $r = 3/4$ convolutional coding and HDD transmitted over a Ricean fading channel with Rayleigh fading pulsed–noise interference $(p = 0.5)$ and AWGN.

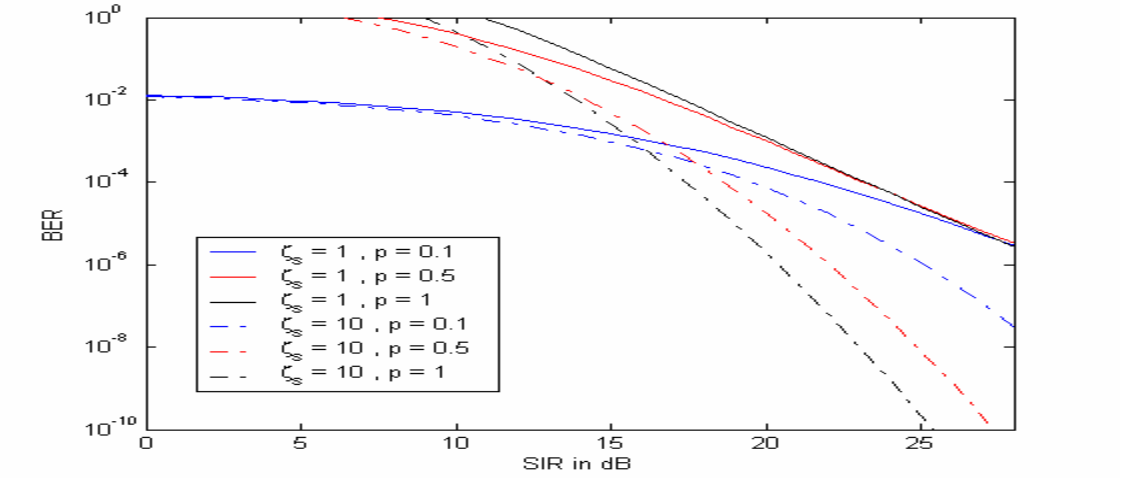

Figure 61. 64–QAM with $r = 3/4$ convolutional coding and HDD transmitted over a Ricean fading channel with Rayleigh fading pulsed–noise interference and AWGN.

Except for the improvement in performance with respect to P_b, the use of convolutional coding with HDD does not alter the picture observed for the non–FEC cases. Performance improves (P_b decreases) with increasing ζ_s. For a low value of ζ_s and for high SIR values, performance is not affected by the parameter *p*. For high values of ζ_s, there is a point in the SIR range beyond which small values of p constitute the worst case for each type of modulation.

E. SUMMARY

This chapter first examined receiver performance when the signal is transmitted over a Rayleigh fading channel with AWGN and Ricean fading, pulsed noise–like interference, both for non–coded and coded signals (HDD only). It was observed that the performance is not significantly affected by the degree of fading of the interference but is affected by the pulsed interference duty cycle, with the worst case being that of continuous interference $(p = 1)$.

Next, the receiver performance when the signal is transmitted over a Ricean fading channel with AWGN and Rayleigh fading pulsed noise–like interference was examined, both for non–coded and coded signals (HDD only). In this case, it was observed that performance is better for weak fading. For strong signal fading, continuous interference (duty cycle of 1) is the worst case, but the interference duty cycle does not affect performance at high SIR. For weaker fading, the interference duty cycle *p* significantly affects performance and, for high SIR, the worst case occurs when the interference duty cycle is low.

V. CONCLUSION

A. FINDINGS

In Chapter III we assumed that the transmitted signal only (and not the pulsed, noise–like interference) was subject to Ricean fading. As expected, we observed that performance deteriorates as the amount of fading encountered by the signal increases. The effect of turning the interference on and off systematically (pulsing) varies depending on the degree of signal fading. For low SIR values, the worst performance occurs for continuous (barrage) interference. For mild fading and higher SIR, the worst performance occurs for low duty cycle pulsing (i.e., when fewer transmitted symbols encounter higher interference power). For stronger fading and higher SIR, the variation of the interference duty cycle does not have any effect on performance. The bound between the low and higher SIR values mentioned here is different for each modulation type.

In Chapter IV we assumed that both the transmitted signal and the interference were subject to Ricean fading, but, due to the complexity of the calculations, two specific cases were examined. In the first one, where the signal is affected by Rayleigh signal fading and the interference by Ricean fading, it was found that the performance is not affected by the degree of interference fading, but it is affected by the interference duty cycle, the worst case being that of continuous interference. In the second case, where Ricean signal fading and Rayleigh interference fading are assumed, findings are similar to those described above for Chapter III.

B. RECOMMENDATIONS FOR FURTHER RESEARCH

The single sub–carrier results of this thesis can be applied in order to evaluate the performance of the complete OFDM system specified in the *IEEE 802.11a* standard under the same channel conditions. The performance of each sub–carrier has to be evaluated independently and the average performance has to be computed. For this to be done, a distribution function for the parameter ζ must be selected, and a value of ζ has to be assigned to each sub–carrier.

Furthermore, the analysis of Chapter IV can be extended to produce an analytical or numerical result for the general case where both the transmitted signal and the interference are subject to Ricean fading. Also, the performance analysis for the specific (simplified) cases investigated in Chapter IV can be extended to include soft decision decoding.

C. CLOSING COMMENTS

The performance analysis of wireless local area networks (WLANs) is of significant importance given their increasing adoption by both military and civilian users. Investigation of their performance under non–favorable conditions (like fading and interference) can help determine an acceptable degree of dependence on WLANs that the users should allow for critical operations.

LIST OF REFERENCES

1. Patrick Count, "Performance analysis of OFDM in frequency-selective, slowly fading Nakagami channels," Master's Thesis, Naval Postgraduate School, Monterey, California, 2001.

2. Irfan Cosa, "Performance of *IEEE 802.11a* wireless LAN standard over frequency-selective, slowly fading Nakagami channels in a pulsed jamming environment," Master's Thesis, Naval Postgraduate School, Monterey, California, 2002.

3. Andreas Tsoumanis, "Performance of the effect of pulsed-noise interference on WLAN signals transmitted over a nakagami fading channel," Master's Thesis, Naval Postgraduate School, Monterey, California, 2004.

4. Chi-han Kao, "Performance of the 802.11a Wireless LAN standard over Frequency-Selective, slow, Ricean Fading Channels," Master's Thesis, Naval Postgraduate School, Monterey, California, 2002.

5. Clark Robertson, Notes for EC4550 (Digital Communications), Naval Postgraduate School, Monterey, California, 2003 (unpublished).

6. Institute of Electrical and Electronics Engineers, *IEEE Std 802.11a-1999, Wireless LAN medium Access Control (MAC) and Physical Layer (PHY) Specifications: High-speed Physical Layer in the 5 GHz Band*, 16 September 1999.

7. Clark Robertson, Notes for EC3510 (Communications Engineering), Naval Postgraduate School, Monterey, California, 2002 (unpublished).

8. Clark Robertson, Notes for EC4580 (Coding and Information), Naval Postgraduate School, Monterey, California, 2003 (unpublished).

9. George C. Clark, Jr. and J. Bibb Cain, *Error-Correction Coding for Digital Communications*, Plenum Press, New York, 1981.

10. I. S. Gradshteyn and I. M. Ryzhik, *Tables of Integrals, Series, and Products*, Academic Press, New York, 1980.

11. Athanasios Papoulis, *Probability, Random Variables and Stochastic Processes*, 2nd edition, McGraw-Hill, New York, 1984.

12. Ramakrishna Janaswamy, *Radiowave Propagation and Smart Antennas for Wireless Communications*, Kluwer Academic Publishers, Norwell, Massachusetts, 2001.

13. J. G. Proakis, *Digital Communications*, 4th ed. McGraw Hill, New York, 2001.

14. B. Sklar, *Digital Communications: Fundamental and Applications*, 2nd ed. Prentice Hall, Upper Saddle River, New Jersey, 2002.

15. Frank Kragh and Clark Robertson, "A general analysis technique for performance of diversity receivers corrupted by partial–band noise interference," MILCOM 2004 (to be published)

INITIAL DISTRIBUTION LIST

1. Defense Technical Information Center
   Ft. Belvoir, Virginia

2. Dudley Knox Library
   Naval Post Graduate School
   Monterey, California

3. Chairman, Code EC/Po
   Department of Electrical and Computer Engineering
   Naval Postgraduate School
   Monterey, California

4. Chairman, Code IS/Bo
   Department of Information Science
   Naval Postgraduate School
   Monterey, California

5. Professor R. Clark Robertson EC/Rc
   Department of Electrical and Computer Engineering
   Naval Postgraduate School
   Monterey, California

6. Professor David C. Jenn , Code EC/Jn
   Department of Electrical and Computer Engineering
   Naval Postgraduate School
   Monterey, California

7. 36 Theod. Voudiklaris Str.
   Evangelos Spyrou
   Chalkis, 34100, Greece